

# 1 **Memory effects on greenhouse gas emissions (CO<sub>2</sub>, N<sub>2</sub>O and CH<sub>4</sub>) following** 2 **grassland restoration?**

3  
4  
5 Lutz Merbold<sup>1,2,\*,#</sup>, Charlotte Decock<sup>3+</sup>, Werner Eugster<sup>1</sup>, Kathrin Fuchs<sup>4</sup>, Benjamin Wolf<sup>4</sup>,  
6 Nina Buchmann<sup>1</sup> and Lukas Hörtnagl<sup>1</sup>

7  
8 <sup>1</sup> Department of Environmental Systems Science, Institute of Agricultural Sciences, Grassland  
9 Sciences Group, ETH Zurich, Universitätsstrasse 2, 8092 Zürich, Switzerland,

10 <sup>2</sup> Mazingira Centre, International Livestock Research Institute (ILRI), Old Naivasha Road, PO  
11 Box 30709, 00100 Nairobi, Kenya

12 <sup>#</sup> now at: Agroscope, Research Division for Agroecology and Environment, Reckenholzstrasse  
13 191, 8046 Zurich, Switzerland

14 <sup>3</sup> Department of Environmental Systems Science, Institute of Agricultural Sciences,  
15 Sustainable Agro-ecosystem Group, ETH Zurich, Universitätsstrasse 2, 8092 Zürich,  
16 Switzerland

17 <sup>+</sup> now at: Department of Natural Resources Management and Environmental Sciences,  
18 California State University, San Luis Obispo, California, USA

19 <sup>4</sup> Institute for Meteorology and Climate Research (IMK-IFU), Karlsruhe Institute of  
20 Technology (KIT), Kreuzeckbahnstrasse 19, 82467 Garmisch-Partenkirchen, Germany

21  
22 \* Correspondence to: lutz.merbold@gmail.com

23  
24  
25 **Keywords:** eddy covariance, global warming potential, manual static chamber, management,  
26 background greenhouse gas emissions, ploughing, fertilization

## 27 28 **Abstract**

29 A five-year greenhouse gas (GHG) exchange study of the three major gas species (CO<sub>2</sub>, CH<sub>4</sub>  
30 and N<sub>2</sub>O) from an intensively managed permanent grassland in Switzerland is presented.  
31 Measurements comprise two years (2010/2011) of manual static chamber measurements of  
32 CH<sub>4</sub> and N<sub>2</sub>O, five years of continuous eddy covariance (EC) measurements (CO<sub>2</sub>/H<sub>2</sub>O – 2010-  
33 2014) and three years (2012-2014) of EC measurement of CH<sub>4</sub> and N<sub>2</sub>O. Intensive grassland

34 management included both regular and sporadic management activities. Regular management  
35 practices encompassed mowing (3-5 cuts per year) with subsequent organic fertilizer  
36 amendments and occasional grazing whereas sporadic management activities comprised  
37 grazing or similar activities. The primary objective of our measurements was to compare pre-  
38 ploughing to post-ploughing GHG exchange and to identify potential memory effects of such  
39 a substantial disturbance on GHG exchange and carbon (C) and nitrogen (N) gains/losses. In  
40 order to include measurements carried out with different observation techniques, we tested two  
41 different measurement techniques jointly in 2013, namely the manual static chamber approach  
42 and the eddy covariance technique for N<sub>2</sub>O, to quantify the GHG exchange from the observed  
43 grassland site.

44 Our results showed that there were no memory effects on N<sub>2</sub>O and CH<sub>4</sub> emissions after  
45 ploughing, whereas the CO<sub>2</sub> uptake of the site considerably increased when compared to post-  
46 restoration years. In detail, we observed large losses of CO<sub>2</sub> and N<sub>2</sub>O during the year of  
47 restoration. In contrast, the grassland acted as a carbon sink under usual management, i.e. the  
48 time periods (2010-2011 and 2013-2014). Enhanced emissions/emission peaks of N<sub>2</sub>O (defined  
49 as exceeding background emissions  $0.21 \pm 0.55 \text{ nmol m}^{-2} \text{ s}^{-1}$  (SE = 0.02) for at least two  
50 sequential days and the seven-day moving average exceeding background emissions) were  
51 observed for almost seven continuous months after restoration as well as following organic  
52 fertilizer applications during all years. Net ecosystem exchange of CO<sub>2</sub> (NEE<sub>CO2</sub>) showed a  
53 common pattern of increased uptake of CO<sub>2</sub> in spring and reduced uptake in late fall. NEE<sub>CO2</sub>  
54 dropped to zero and became positive after each harvest event. Methane (CH<sub>4</sub>) exchange  
55 fluctuated around zero during all years. Overall, CH<sub>4</sub> exchange was of negligible importance  
56 for both, the GHG budget as well as for the carbon budget of the site.

57 Our results stress the inclusion of grassland restoration events when providing cumulative sums  
58 of C sequestration potentials and/or global warming potentials (GWPs). Consequently, this  
59 study further highlights the need for continuous long-term GHG exchange observations as well  
60 as the implementation of our findings into biogeochemical process models to track potential  
61 GHG mitigation objectives as well as to predict future GHG emission scenarios reliably.

62  
63  
64  
65  
66  
67

## 68 **1 Introduction**

69

70 Grassland ecosystems are commonly known for their provisioning of forage, either directly via  
71 grazing of animals on site, or indirectly by regular biomass harvest and preparation of silage  
72 or hay. Simultaneously, grasslands have further been acknowledged for their greenhouse gas  
73 (GHG) mitigation and soil carbon sequestration potential (Lal, 2004; Smith et al., 2008).  
74 However, greenhouse gas emissions from grasslands, particularly N<sub>2</sub>O and CH<sub>4</sub> have been  
75 shown to offset net carbon dioxide equivalent (CO<sub>2</sub>-eq.) gains (Ammann et al., 2020; Dengel  
76 et al., 2011; Hörtnagl et al., 2018; Hörtnagl and Wohlfahrt, 2014; Merbold et al., 2014; Schulze  
77 et al., 2009). Still, datasets containing continuous measurements of all three major GHGs (CO<sub>2</sub>,  
78 CH<sub>4</sub> and N<sub>2</sub>O) in grassland ecosystems remain limited (Hörtnagl et al., 2018), include a single  
79 GHG only, or focus on specific management activities (Fuchs et al., 2018; Krol et al., 2016).  
80 At the same time such datasets are extremely valuable by providing key training datasets for  
81 biogeochemical process models (Fuchs et al., 2020a).

82 Here we investigate the GHG exchange of the three major trace gases (CO<sub>2</sub>, CH<sub>4</sub> and N<sub>2</sub>O)  
83 over five consecutive years in a typical managed grassland on the Swiss plateau. Our study  
84 includes the application of traditional GHG chamber measurements and state-of-the-art GHG  
85 concentration measurements with a quantum cascade laser absorption spectrometer and a sonic  
86 anemometer in an eddy covariance setup (Eugster and Merbold, 2015). Prior to our  
87 measurements we hypothesized short-term losses of CO<sub>2</sub> and more continuous losses of  
88 primarily N<sub>2</sub>O following dramatic managements events such as ploughing occurring at  
89 irregular time intervals. We further hypothesized an increased carbon uptake strength  
90 compared to the pre-ploughing years. Methane emissions were hypothesized to be of minor  
91 importance due to the limited time of grazing animals on site (Merbold et al., 2014).

92 Up to date the majority of greenhouse gas exchange research has focused on CO<sub>2</sub>, with less  
93 focus on the other two important GHGs N<sub>2</sub>O and CH<sub>4</sub>, even though an increased interest in  
94 these other gas species has become visible in recent years (Ammann et al., 2020; Ball et al.,  
95 1999; Cowan et al., 2016; Krol et al., 2016; Kroon et al., 2007, 2010; Necpálová et al., 2013;  
96 Rutledge et al., 2017). The existing exceptions are often referred to as “high-flux” ecosystems,  
97 namely wetlands and livestock production system in terms of CH<sub>4</sub> (Baldocchi et al., 2012;  
98 Felber et al., 2015; Laubach et al., 2016; Teh et al., 2011) and agricultural ecosystems such as  
99 bioenergy system with considerable N<sub>2</sub>O emissions (Cowan et al., 2016; Fuchs et al., 2018;  
100 Krol et al., 2016; Skiba et al., 1996, 2013; Wecking et al., 2020; Zenone et al., 2016; Zona et

101 al., 2013). Agricultural ecosystems and specifically grazed systems are characterized by GHG  
102 emissions caused through anthropogenic activities. These activities lead to changes in GHG  
103 emission patterns and include harvests, amendments of fertilizer and/or pesticides and less  
104 frequently occurring ploughing, harrowing and re-sowing events. While ploughing has been  
105 shown to lead to considerable short-term emissions of CO<sub>2</sub> and N<sub>2</sub>O (Buchen et al., 2017;  
106 Cowan et al., 2016; Hörtnagl et al., 2018; MacKenzie et al., 1997; Merbold et al., 2014;  
107 Rutledge et al., 2017; Vellinga et al., 2004), regular harvests have been shown to lead to  
108 increased CO<sub>2</sub> uptake (Zeeman et al., 2010) and grazing leads to large CH<sub>4</sub> emissions (Dengel  
109 et al., 2011; Felber et al., 2015). Other studies showed contrary results with reduced N<sub>2</sub>O  
110 emissions following ploughing of a drained grassland when compared to a fallow in Canada  
111 (MacDonald et al., 2011).

112 Still, the full range of management activities occurring in intensively managed grasslands and  
113 their respective impact on GHG exchange has not been investigated in detail. In a recent  
114 synthesis including grasslands located along an altitudinal gradient in Central Europe, Hörtnagl  
115 et al. (2018) highlighted the most important abiotic drivers of CO<sub>2</sub> (light, water availability and  
116 temperature), CH<sub>4</sub> (soil water content, temperature and grazing) and N<sub>2</sub>O exchange (water  
117 filled pore space and soil temperature). The study by Hörtnagl et al. (2018) further elaborated  
118 the variation in management intensity and related variations in GHG exchange across sites,  
119 stressing the need for more case studies based on continuous GHG observations to improve  
120 existing knowledge and close remaining knowledge gaps. To complete the picture on factors  
121 driving ecosystem GHG exchange, irregular occurring events such as dry spells or  
122 extraordinary wet periods can further lead to enhanced or reduced GHG emissions (Chen et al.,  
123 2016; Hartmann and Niklaus, 2012; Hopkins and Del Prado, 2007; Mudge et al., 2011; Wolf  
124 et al., 2013).

125 While drought has been shown to reduce CO<sub>2</sub> uptake in forests (Ciais et al., 2005) whereas  
126 dry spells did not affect CO<sub>2</sub> uptake in grasslands (Wolf et al., 2013), flooding leads primarily  
127 to enhanced CH<sub>4</sub> emissions (Knox et al., 2015) and large precipitation events can lead to  
128 plumes of N<sub>2</sub>O (Fuchs et al., 2018; Zona et al., 2013) similar to freeze-thaw events (Butterbach-  
129 Bahl et al., 2011; Matzner and Borken, 2008) to name only some examples. Consequently,  
130 understanding both, anthropogenic impacts such as management besides environmental  
131 impacts on ecosystem GHG exchange, are crucially important to suggest appropriate climate  
132 change mitigation as well as adaptation strategies for future land management with ongoing  
133 climate change.

134 Different measurement techniques to quantify the net GHG exchange in ecosystems are known  
135 and the most common approaches are either GHG chamber measurements or the eddy  
136 covariance (EC) technique. Static manual chamber measurements have been used for more  
137 than a century to quantify CO<sub>2</sub> emissions (Lundegardh, 1927) and their application has further  
138 been expanded during the last decades to quantify losses of the three major GHGs, CO<sub>2</sub>, N<sub>2</sub>O  
139 and CH<sub>4</sub> from soils (Imer et al., 2013; Pavelka et al., 2018a; Pumpanen et al., 2004; Rochette  
140 et al., 1997). Even though more complex in technology and assumptions made before carrying  
141 out measurements, the eddy covariance (EC) technique has become a valuable tool to derive  
142 ecosystem integrated CO<sub>2</sub> and H<sub>2</sub>O<sub>vapour</sub> exchange across the globe (Baldocchi, 2014; Eugster  
143 and Merbold, 2015). The technique has been further extended to continuous measurements of  
144 CH<sub>4</sub> and N<sub>2</sub>O with the development of easy field-deployable fast-response analyzers during  
145 the last decade (Brümmer et al., 2017; Felber et al., 2015; Kroon et al., 2007; Nemitz et al.,  
146 2018a; Wecking et al., 2020). Each of the two approaches has its strengths and weaknesses and  
147 it is beyond the scope of this study to discuss each of them in detail. However, we refer to a set  
148 of reference papers highlighting the advantages and disadvantages of each technique separately  
149 (chambers: (Ambus et al., 1993; Brümmer et al., 2017; Pavelka et al., 2018a); eddy covariance:  
150 (Baldocchi, 2014; Denmead, 2008; Eugster and Merbold, 2015; Nemitz et al., 2018)).  
151 The overall objective of this study was to investigate the net GHG exchange (CO<sub>2</sub>, CH<sub>4</sub> and  
152 N<sub>2</sub>O) before and after grassland restoration and thus fill existing knowledge gaps caused by  
153 limited amounts of available GHG exchange data from intensively managed grasslands. The  
154 specific goals were: (i) to assess pre- and post-ploughing GHG exchange in a permanent  
155 grassland in central Switzerland accounting for changes in GHG exchange following frequent  
156 management activities; (ii) to compare two different measurement techniques, namely eddy  
157 covariance and static greenhouse gas flux chambers to quantify the GHG exchange in a  
158 business-as-usual year; and (iii) to provide a five year GHG budget of the site and quantify  
159 losses/gains of C and N. Based on our results we provide suggestions for future research  
160 approaches to further understand ecosystem GHG exchange, to mitigate GHG emissions and  
161 to ensure nutrient retention at the site for sustainable production from permanent grasslands in  
162 the future.

163  
164  
165  
166  
167

## 168 **2 Material and Methods**

### 169 **2.1 Study site**

170 The Chamau grassland site (Fluxnet identifier - CH-Cha) is located in the pre-alpine lowlands  
171 of Switzerland at an altitude of 400 m a.s.l. (47°12' 37"N, 8°24'38"E) and characterized by  
172 intensive management (Zeeman et al., 2010). The site is divided into two parcels (Parcel A and  
173 B) with occasionally slightly different management regimes [see also *Fuchs et al., 2018*]. Mean  
174 annual temperature (MAT) is 9.1 °C, and mean annual precipitation (MAP) is 1151 mm. The  
175 soil type is a Cambisol with a pH ranging between 5 and 6, a bulk density between 0.9 and 1.3  
176 kg m<sup>-3</sup> and a carbon stock of 55.5–69.4 t C ha<sup>-1</sup> in the upper 20 cm of the soil. The common  
177 species composition consists of Italian ryegrass (*Lolium multiflorum*) and white clover  
178 (*Trifolium repens L.*). For more details of the site we refer to Zeeman et al., (2010).

179 CH-Cha is intensively managed, with activities being either recurrent – referred to as  
180 usual/regular - or sporadic. Usual management refers to regular mowing and subsequent  
181 organic fertilizer application in form of liquid slurry (up to 7 times per year). In addition, the  
182 site is occasionally grazed by sheep and cattle for few days in early spring and/or fall (H.-R.  
183 Wettstein personal communication, Table S1). Sporadic activities aim at maintaining the  
184 typical fodder species composition and comprise reseeding, herbicide and pesticide application  
185 or irregular ploughing and harrowing on an approximately decadal timescale (Merbold et al.,  
186 2014). By such activity, mice are eradicated and a high-quality sward for fodder production is  
187 re-established following weed contamination. Specific information on management activity  
188 (timing, type of management, amount of biomass harvested) were reported by the farmers on  
189 site (Table S1). Additionally, representative samples of organic fertilizer were collected shortly  
190 before fertilizer application events and sent to a central laboratory for nutrient content analysis  
191 (Labor fuer Boden- und Umweltanalytik, Eric Schweizer AG, Thun, Switzerland). Harvest  
192 estimates were compared to estimates based on destructive sampling of randomly chosen plots  
193 (n = 10) in the years 2010, 2011, 2013 and 2014. The amount of harvested biomass in the year  
194 2012 was based on a calibration of the values presented by the farmer in comparison to the on-  
195 site destructive harvests in previous and following years (Table S1).

196

### 197 **2.2 Eddy covariance flux measurements**

#### 198 *2.2.1 Eddy covariance setup*

199 The specific site characteristics with two prevailing wind directions (North-northwest and  
200 South-south east) allows continuous observations of both management parcels. It is

201 noteworthy, that the separation of the two parcels is done exactly at the location of the tower.  
202 See Zeeman et al. (2010) and Fuchs et al. (2018) for further details. The eddy covariance setup  
203 consisted of a three-dimensional sonic anemometer (2.4 m height, Solent R3, Gill Instruments,  
204 Lymington, UK), an open-path infrared gas analyzer (IRGA, LI-7500A, LiCor Biosciences,  
205 Lincoln, NE, USA) to measure the concentrations of CO<sub>2</sub> and H<sub>2</sub>O<sub>vapour</sub> and a recently  
206 developed continuous-wave quantum cascade laser absorption spectrometer (mini-QCLAS -  
207 CH<sub>4</sub>, N<sub>2</sub>O, H<sub>2</sub>O configuration, Aerodyne Research Inc., Billerica, MA, USA) to measure the  
208 concentrations of CH<sub>4</sub>, N<sub>2</sub>O, and H<sub>2</sub>O<sub>vapour</sub>. 3D wind components (u, v, w), CO<sub>2</sub> and H<sub>2</sub>O<sub>vapour</sub>  
209 concentration data from the IRGA were collected at a 20 Hz time interval, whereas  
210 concentrations of CH<sub>4</sub> and N<sub>2</sub>O were collected at a 10 Hz rate from the QCLAS. The QCLAS  
211 provided the dry mole fraction for both trace gases (CH<sub>4</sub> and N<sub>2</sub>O), and data were transferred  
212 to the data acquisition system (MOXA embedded Linux computer, Moxa, Brea, CA, USA) via  
213 an RS-232 serial data link and merged with the sonic anemometer and IRGA data streams in  
214 near-real time (Eugster and Plüss, 2010). Important to note is that the QCLAS was stored in a  
215 temperature-controlled box (temperature variation during the course of a single day was  
216 reduced to < 2 K) and located approximately 4 meters away from the EC tower to avoid long  
217 tubing. Total tube length from the inlet near the sonic anemometer to the measurement cell was  
218 6.5 m. The inlet consisted of a coarse sinter filter (common fuel filter used in model cars) and  
219 a fine vortex filter (mesh size 0.3µm and a water trap) installed directly before the QCLAS.  
220 Filters were changed monthly or if the cell pressure in the laser dropped by more than 2 torr.  
221 Flow rate of approximately 15 l min<sup>-1</sup> was achieved with a large vacuum pump (BOC Edwards  
222 XDS-35i, USA and TriScoll 600, Varian Inc., USA – the latter was used during maintenance  
223 of the Edwards pump). The pumps were maintained annually and replaced twice due to  
224 malfunction during the observation period. The infrared gas analyzer was calibrated to known  
225 concentrations of CO<sub>2</sub> and H<sub>2</sub>O each year. The QCLAS did not need calibration due to its  
226 operating principles, and an internal reference cell (mini-QCL manual, Aerodyne Research  
227 Inc., Billerica, MA, USA) eased finding the absorption spectra after each restart of the analyzer.

228

### 229 *2.2.2 Eddy covariance flux processing, post-processing and quality control*

230 Raw fluxes of CO<sub>2</sub>, CH<sub>4</sub>, N<sub>2</sub>O ( $F_{GHG}$ , µmol m<sup>-2</sup> s<sup>-1</sup>) were calculated as the covariance between  
231 turbulent fluctuations of the vertical wind speed and the trace gas species mixing ratio,  
232 respectively (Baldocchi, 2003; Eugster and Merbold, 2015). Open-path infrared gas analyzer  
233 (IRGA) CO<sub>2</sub> measurements were corrected for water vapor transfer effects (Webb et al., 1980).  
234 A 2-dimensional coordinate rotation was performed to align the coordinate system with the

235 mean wind streamlines so that the vertical wind vector  $\dot{w} = 0$ . Turbulent departures were  
236 calculated by Reynolds (block) averaging of 30 min data blocks. Frequency response  
237 corrections were applied to raw fluxes, accounting for high-pass and low-pass filtering for the  
238 CO<sub>2</sub> signal based on the open-path IRGA as well as for the closed-path CH<sub>4</sub> and N<sub>2</sub>O data  
239 (Fratini et al., 2014). All fluxes were calculated using the software *EddyPro* (version 6.0, LiCor  
240 Biosciences, Lincoln, NE, USA) (Fratini and Mauder, 2014).

241 The quality of half-hourly raw time series was assessed during flux calculations following  
242 (Vickers and Mahrt, 1997). Raw data were rejected if (a) spikes accounted for more than 1 %  
243 of the time series, (b) more than 10 % of available data points were significantly different from  
244 the overall trend in the 30 min time period, (c) raw data values were outside a plausible range  
245 ( $\pm 50 \mu\text{mol m}^{-2} \text{s}^{-1}$  for CO<sub>2</sub>,  $\pm 300 \text{ nmol m}^{-2} \text{s}^{-1}$  for N<sub>2</sub>O and  $\pm 1 \mu\text{mol m}^{-2} \text{s}^{-1}$  for CH<sub>4</sub>) and (d)  
246 window dirtiness of the IRGA sensor exceeded 80 %. Only raw data that passed all quality  
247 tests were used for flux calculations.

248 Half-hourly flux data were rejected if (e) fluxes were outside a physically plausible range (ie.  
249  $\pm 50 \mu\text{mol m}^{-2} \text{s}^{-1}$  for CO<sub>2</sub>) (f) the steady state test exceeded 30 % and (g) the developed  
250 turbulent conditions test exceeded 30 % (Foken et al., 2006). Between 1<sup>st</sup> January 2010 and  
251 31<sup>st</sup> December 2014 64572 (88% of all possible data) 30-min flux values were calculated for  
252 CO<sub>2</sub>, of which 42865 (57.8%) passed all quality tests and were used for analyses in the present  
253 study (Table 1). The amount of available flux values for N<sub>2</sub>O and CH<sub>4</sub> were less, since we were  
254 only capable to continuously measure both gases from 2012 onwards (Table 1). Flux values in  
255 this manuscript are given as number of moles of matter/mass per ground surface area and unit  
256 time. Negative fluxes represent a flux of a specific gas species from the atmosphere into the  
257 ecosystem, whereas positive fluxes represent a net loss from the system.

258

## 259 **2.3 Static greenhouse gas flux chambers**

### 260 *2.3.1 Manual static GHG chamber setup*

261 Static manual opaque GHG chambers were installed within the footprint of the site to measure  
262 soil fluxes in 2010 and 2011 (n =16) as well as during summer 2013 (n = 10). The chambers  
263 were made of polyvinyl chloride tubes with a diameter of 0.3 m (Imer et al., 2013). The average  
264 headspace height was  $0.136 \text{ m} \pm 0.015 \text{ m}$  and average insertion depth of the collars into the  
265 soil was  $0.08 \text{ m} \pm 0.05 \text{ m}$ . During sampling days with vegetation larger than 0.3 m inside the  
266 chamber, collar extensions (0.45 m) were used (2013 only). Chamber lids were equipped with  
267 reflective aluminium foil to minimize heating inside the chamber during the period of actual  
268 measurement. Spacing between the chambers was approximately seven m and an equal number



269 of chambers were installed in each parcel. For further details we refer to Imer et al. (2013).  
270 Chamber measurements were carried out on a weekly basis during the growing season in all  
271 three years (2010, 2011 and 2013), and at least once a month during the winter season in 2010  
272 and 2011. More frequent measurements of N<sub>2</sub>O emissions (every day) were performed  
273 following fertilization events in 2013 for seven consecutive days after each event. Besides this,  
274 an intensive measurement campaign lasting 48 hours (two-hour measurement interval) was  
275 carried out in September 2010.

276

### 277 *2.3.2 GHG concentrations measurements*

278 During each chamber closure four gas samples were taken, one immediately after closure and  
279 then in approximately ten-minute time increments. With this approach, we guaranteed that the  
280 chambers were closed no longer than 40 minutes to avoid potential saturation effects. Syringes  
281 (60 ml volume) were inserted into the chambers lid septa to take the gas samples. The collected  
282 air sample was injected into pre-evacuated 12 ml vials (Labco Limited, Buckinghamshire, UK)  
283 in the next step. Prior to the second, third and fourth sampling of each chamber, the air in  
284 chamber headspace was circulated with the syringe volume of air from the chamber headspace  
285 to minimize effects of built-up concentration gradients inside the chamber.

286 Gas samples were analyzed for their respective CO<sub>2</sub>, CH<sub>4</sub> and N<sub>2</sub>O concentrations in the lab as  
287 soon as possible after sample collection and not stored for more than a few days. Gas sample  
288 analysis was performed with a gas chromatograph (Agilent 6890 equipped with a flame  
289 ionization detector, a methanizer - Agilent Technologies Inc., Santa Clara, USA - and an  
290 electron capture detector – SRI Instruments Europe GmbH, 53604 Bad Honnef, Germany) as  
291 described by Hartmann and Niklaus (2012).

292

### 293 *2.3.3 GHG chamber flux calculations and quality control*

294 GHG fluxes were calculated based on the rate of gas concentration change inside the chamber  
295 headspace. Data processing, which included flux calculation and quality checks, was carried  
296 out with the statistical software R (R Development Core Team, 2010). Thereby the rate of  
297 change was calculated by the slope of the linear regression of gas concentration over time. Flux  
298 calculation was based on the common equation containing GHG concentration ( $c$  in nmol mol<sup>-1</sup>  
299 <sup>1</sup> for CH<sub>4</sub> and N<sub>2</sub>O), time ( $t$  in seconds), atmospheric pressure ( $p$  in Pa), the headspace volume  
300 ( $V$  in m<sup>-3</sup>), the universal gas constant ( $R = 8.3145 \text{ m}^3 \text{ Pa K}^{-1} \text{ mol}^{-1}$ ), ambient air temperature  
301 ( $T_a$  in K) and the surface area enclosed by the chamber ( $A$  in m<sup>-2</sup>) (equation 1 in Imer et al.  
302 (2013)).

303 Flux quality criteria were based on the fit of the linear regression. If the correlation coefficient  
304 of the linear regression ( $r^2$ ) was  $< 0.8$  the actual flux value was rejected from the subsequent  
305 data analysis (see Imer et al. 2013 for further details on data quality control, and Table 1).  
306 Furthermore, if the slope between the 1<sup>st</sup> and 2<sup>nd</sup> GHG concentration measurement deviated  
307 considerably from the following concentrations we omitted the first value and calculated the  
308 flux based on three instead of four samples. Mean chamber GHG fluxes were then calculated  
309 as the arithmetic mean of all available individual chamber fluxes for each date. A total of 35  
310 GHG flux calculations ( $\text{CH}_4$  and  $\text{N}_2\text{O}$ ) were available for the years 2010 and 2011. Another 52  
311  $\text{N}_2\text{O}$  flux values were available for the five-month peak-growing season in 2013.

312

#### 313 *2.4 Gapfilling and annual sums of $\text{CO}_2$ , $\text{CH}_4$ , and $\text{N}_2\text{O}$*

314 To date a common strategy to fill gaps in EC data of  $\text{CH}_4$  and  $\text{N}_2\text{O}$  has not been agreed on. The  
315 commonly used methods are simple linear approaches (Mishurov and Kiely, 2011) or the  
316 application of more sophisticated tools such as artificial neural networks (Dengel et al., 2011).  
317 The difficulty of finding an adequate gap-filling strategy results from the fact that emission  
318 pulses of either  $\text{N}_2\text{O}$  or  $\text{CH}_4$  remain challenging to predict. Similarly, different measurement  
319 approaches – i.e. low temporal resolution manual GHG chambers compared to high temporal  
320 resolution eddy covariance measurements - need different gap-filling approaches (Mishurov  
321 and Kiely, 2011; Nemitz et al., 2018). In order to keep the gap-filling methods as simple and  
322 reliable as possible, we used a running median (30 and 60 days for eddy covariance based and  
323 chamber  $\text{N}_2\text{O}$  fluxes, respectively). A similar approach was recently chosen by Hörtnagl et al.  
324 (2018) due to its reduced sensitivity to peaks in the  $\text{N}_2\text{O}$  exchange data. The approach was  
325 particularly chosen as it minimizes the bias occurring from linear gap filling or simply using  
326 an overall average value. While the gapfilling approach may be of less importance for EC flux  
327 measurements with its high temporal data availability, it is the more important for less  
328 frequently available GHG fluxes derived via manual chambers. Given the occurrence of  
329 sporadic  $\text{N}_2\text{O}$  peaks which occur mostly in relation to management activities and last for few  
330 hours/days only as well as the labour needed to carry out GHG chambers measurements,  
331 researchers commonly aim at having weekly or biweekly flux data (i.e. Imer et al. 2013). The  
332 respective sampling design is commonly designed to capture potential  $\text{N}_2\text{O}$  flux peaks as well  
333 as some background values (Mishurov and Kiely, 2011). If one then uses either a linear  
334 interpolation or an overall average value, one can derive a budget which is than a likely  
335 overestimation of the annual flux budget caused by the few flux peaks observed in such  
336 managed systems. The same bias is likely to occur if just flux averages are used since few very

337 high emission peaks will affect such an average. Thus, and in order to simulate N<sub>2</sub>O emission  
338 peaks more reliably, we have chosen the approach as taken by Hörtnagl et al. (2018).

339 In contrast to CH<sub>4</sub> and N<sub>2</sub>O various well-established approaches to fill CO<sub>2</sub> flux data exist  
340 (Moffat et al., 2007). Here, we filled gaps in CO<sub>2</sub> exchange data following the marginal  
341 distribution sampling method (Reichstein et al., 2005) which was implemented in the R  
342 package REddyProc (<https://r-forge.r-project.org/projects/reddyproc/>).

343 Calculation of the global warming potential (GWP) given in CO<sub>2</sub>-equivalents followed the  
344 recommendations given in the 5<sup>th</sup> Assessment Report of the Intergovernmental Panel on  
345 Climate Change (IPCC), with CH<sub>4</sub> having a 28 and N<sub>2</sub>O a 265 times greater GWP than CO<sub>2</sub>  
346 on a per mass basis over a time horizon of 100 years (Stocker et al., 2013).

347

### 348 *2.5 Meteorological and phenological data*

349 Flux measurements were accompanied by standard meteorological measurements. These  
350 included observations of soil temperature (depths of 0.01, 0.02, 0.05, 0.10, and 0.15 m, TL107  
351 sensors, Markasub AG, Olten, Switzerland), soil moisture (depths of 0.02 and 0.15 m, ML2x  
352 sensors, Delta-T Devices Ltd., Cambridge, UK) and air temperature (2 m height, Hydroclip S3  
353 sensor, Rotronic AG, Switzerland). Furthermore, we measured the radiation balance including  
354 short-wave incoming and outgoing radiation, long-wave incoming and outgoing radiation  
355 (CNR1 sensor with ventilated Markasub housing, Kipp and Zonen, Delft, the Netherlands) as  
356 well as photosynthetically active radiation at 2 m height (PARlite sensor, Kipp and Zonen,  
357 Delft, the Netherlands). All data were stored as 30 min averages on a datalogger in a climate-  
358 controlled box on site (CR10X, Campbell Scientific, Logan, UT, USA).

359

360

361

362

363

364

365

366

367

368

369

370

### 371 **3 Results**

#### 372 *3.1 General site conditions*

373 The Chamau study site (CH-Cha) experienced meteorological conditions typical for the site  
374 during the five-year observation period. Summer precipitation commonly exceeded winter  
375 precipitation (Figure 1a). A spring drought was recorded from March till May 2011 (Wolf et  
376 al., 2013), leading to considerably lower soil water content than in previous and following years  
377 (Figure 1a). Average daily air temperatures rose up to 26.7 °C (27<sup>th</sup> July 2013) during summer  
378 and average daily temperature in winter dropped as low as -12.7 °C (6<sup>th</sup> February 2012, Figure  
379 1b) with soil temperature following in a dampened pattern (Figure 1b). Average daily  
380 photosynthetic photon flux density did not differ considerably over the five-year observation  
381 period (Figure 1c). The site rarely experienced snow cover during winter (Figure 1b).

382 The complexity in management activities becomes apparent when comparing business as usual  
383 years (e.g. 2011) with the restoration year (2012, Figure 2a and b), highlighting the importance  
384 of grassland restoration to maintain productivity yields. Prior to 2012 an obvious decline in  
385 productivity with larger C and N inputs was found compared to the outputs in the years after  
386 restoration (2013 and 2014, Figure 2a and b).

387

#### 388 *3.2 EC N<sub>2</sub>O fluxes vs. chamber derived N<sub>2</sub>O fluxes*

389 In 2013, we had the chance of comparing N<sub>2</sub>O fluxes measured with two considerably different  
390 GHG measurement techniques, namely eddy covariance and static chambers. The chambers  
391 (n=10) were installed within the EC footprint. Our results reveal a similar temporal pattern,  
392 with increased N<sub>2</sub>O losses being captured by both methodologies following fertilizer  
393 application. However, we could not identify a consistent bias of either technique (Figure 3a).  
394 Direct comparison of both measurements revealed a reasonable correlation (slope  $m = 0.61$ ,  $r^2$   
395  $= 0.4$ ) and larger variation between both techniques with increasing flux values (Figure 3b).

396

#### 397 *3.3 Temporal variation of GHG exchange*

398 Fluxes of CO<sub>2</sub> and N<sub>2</sub>O showed considerable variation between and within years. This variation  
399 primarily occurs due to management activities and seasonal changes in meteorological  
400 variables (Figures 1 and 4). In contrast, methane fluxes did not show a distinct seasonal pattern.

401

402

403

404 *CO<sub>2</sub> exchange*

405 In pre-ploughing years (2010 and 2011), the Chamau site showed 60 % lower CO<sub>2</sub> uptake  
406 compared to the post-ploughing years (2013 and 2014, Table 2). All four non-ploughing years  
407 revealed largest CO<sub>2</sub> uptake rates in late spring (daily averaged peak uptake rates were >10  
408  $\mu\text{mol CO}_2 \text{ m}^{-2} \text{ s}^{-1}$ , March and April, Figure 4a). Besides the seasonal effects a clear impact of  
409 harvest events could be identified, with abrupt changes from net uptake of CO<sub>2</sub> to either  
410 reduced uptake or net loss of CO<sub>2</sub> (light blue arrows indicate harvest event, Figure 4a). A  
411 similar but less pronounced effect was found following grazing periods (light and dark brown  
412 arrow, Figure 4a). A complete switch from net uptake to net CO<sub>2</sub> release was observed during  
413 the first three months of 2012, after ploughing and during re-cultivation of the grassland. In  
414 this specific year, the site only experienced snow cover for few days (Figure 1c) and  
415 temperatures below 5 °C occurred more regularly than in all other years (Figure 1 b). Seasonal  
416 CO<sub>2</sub> exchange was characterized by net release of CO<sub>2</sub> in winter (DJF), highest CO<sub>2</sub> uptake  
417 rates were observed in spring (MAM), constant uptake rates during summer (JJA) which  
418 however were lower than those measured in spring, and very low net release of CO<sub>2</sub> in fall  
419 (Table 3). Average winter CO<sub>2</sub> exchange for the five-year observation period (gap-filled 30  
420 min data) was  $0.28 \pm 5.68 \mu\text{mol CO}_2 \text{ m}^{-2} \text{ s}^{-1}$  (SE = 0.04, Table 3). The restoration year 2012  
421 showed a slightly different pattern with relatively large CO<sub>2</sub> release in winter and spring and  
422 considerably lower uptake rates in summer. The years before the restoration (2010 and 2011)  
423 were characterized by smaller net uptake rates during spring and summer when compared to  
424 the post-ploughing years (2013 and 2014). Additionally, winter fluxes in 2010 and 2011 were  
425 positive (net release of CO<sub>2</sub>), while winter fluxes in the years 2013 and 2014 were showing a  
426 small but consistent net uptake of CO<sub>2</sub> (Figure 4a, Table 3).

427

428 *CH<sub>4</sub> exchange*

429 The individual static chamber measurements (2011&2011) were often below the detection  
430 limit and fluctuated around zero similar to the eddy covariance measurements (Figure 4b). Any  
431 methane peaks expected due to freezing and thawing in late winter and early spring were not  
432 observed. Also, commonly reported net emissions of methane during grazing of animals were  
433 not seen (Figure 4b). Seasonal differences of methane exchange did not show a clear pattern  
434 (Table 3). A comparison of methane fluxes obtained by both, static GHG chambers and EC  
435 measurements as done for N<sub>2</sub>O (see next paragraph) could not be performed due to a  
436 malfunction of the respective detector in the gas chromatograph.

437

### 438 *N<sub>2</sub>O exchange*

439 N<sub>2</sub>O exchange was low during the majority of the days over the five-year observation period,  
440 fluctuating around zero (Figure 4c). However, clear peaks in N<sub>2</sub>O emissions were observed  
441 following fertilization events or periods with high rainfall after a dry period in summer (i.e.  
442 summer 2013 and 2014, Figures 3a and 4c). While event driven N<sub>2</sub>O emissions were commonly  
443 on the order of 4 to 8 nmol N<sub>2</sub>O m<sup>-2</sup> s<sup>-1</sup> (Figure 4c), N<sub>2</sub>O emissions following ploughing and  
444 subsequent re-sowing of the grassland in 2012 lead to up to three times as high N<sub>2</sub>O emissions  
445 (Figure 4c, year 2012, see also Merbold et al. (2014)). Similar to methane, enhanced N<sub>2</sub>O  
446 emissions in late winter or early spring as reported by other studies could not be identified  
447 (Figure 4c).

448 Background N<sub>2</sub>O fluxes were estimated by analysing all high temporal resolution flux data but  
449 excluding the restoration year 2012 and all values one week after a management event. Daily  
450 average background fluxes were  $0.21 \pm 0.55$  nmol m<sup>-2</sup> s<sup>-1</sup> (SE = 0.02). Differences in N<sub>2</sub>O  
451 exchange over the course of individual years became obvious when splitting the dataset into  
452 the four seasons (winter – DJF, spring – MAM, summer – JJA and fall – SON). In contrast to  
453 CO<sub>2</sub> exchange that showed large net uptake rates in spring, N<sub>2</sub>O emissions were largest during  
454 summer (JJA) and lowest in winter (DJF). As highlighted for the other gases, the year of  
455 grassland restoration showed a completely different picture (Table 3).

456

### 457 *3.4 Annual sums and Global Warming Potential (GWP) of CO<sub>2</sub>, CH<sub>4</sub> and N<sub>2</sub>O*

458 Annual sums showed a net uptake of CO<sub>2</sub> during the two pre-ploughing years  
459 (-695 g CO<sub>2</sub> m<sup>-2</sup> yr<sup>-1</sup> and -978 g CO<sub>2</sub> m<sup>-2</sup> yr<sup>-1</sup> in 2010 and 2011 respectively). Up to three times  
460 of this net uptake was reached in 2013 and 2014, the two post-ploughing years (-2046 g CO<sub>2</sub>  
461 m<sup>-2</sup> yr<sup>-1</sup> and -2751 g CO<sub>2</sub> m<sup>-2</sup> yr<sup>-1</sup>, Table 2). In contrast, the ploughing year 2011 was  
462 characterized by a net release of CO<sub>2</sub> (1447 g CO<sub>2</sub> m<sup>-2</sup> yr<sup>-1</sup>).

463 Methane budgets for the years 2010 and 2011 were not be calculated as many of the available  
464 measurements were below the limit of detection. For the years 2012 – 2014, the annual methane  
465 budget showed a minor release of 26.8 – 55.2 g CH<sub>4</sub> m<sup>-2</sup> yr<sup>-1</sup>.

466 The Chamau site was characterized by a net release of nitrous oxide over the five-year study  
467 period. While annual average N<sub>2</sub>O emissions ranging between 0.34 and 1.17 g N<sub>2</sub>O m<sup>-2</sup> yr<sup>-1</sup> in  
468 the non-ploughing years, the site emitted 4.36 g N<sub>2</sub>O m<sup>-2</sup> yr<sup>-1</sup> in 2012. As an important note,  
469 due to the limited data availability for the years 2010 and 2011, the budgets of those years are  
470 likely incomplete.

471 The global warming potential (GWP), expressed as the yearly cumulative sum of all gases after  
472 their conversion to CO<sub>2</sub>-equivalents, was negative during all years (between -387 and -2577  
473 CO<sub>2</sub>-eq. m<sup>-2</sup>) except for the ploughing year 2012 (+2629 CO<sub>2</sub>-eq. m<sup>-2</sup>).

474 Overall, CO<sub>2</sub> exchange contributed more than 90% to the total GHG balance in 2011, 2013 and  
475 2014. Clearly, CH<sub>4</sub> exchange was of minimal importance for the GHG budget (Table 2). In  
476 2010, the contribution of CO<sub>2</sub> to the site's GHG budget was almost 70%, and N<sub>2</sub>O contributed  
477 about 30%. Only in 2012, the year of restoration, CO<sub>2</sub> and N<sub>2</sub>O exchange contributed almost  
478 equally to the site's overall GHG budget (55.1% and 43.9%, respectively).

479

### 480 *3.5. Carbon gains/losses of the Chamau site between 2010 and 2014*

481 The Chamau site assimilated on average  $-441 \pm 260$  g CO<sub>2</sub>-C m<sup>-2</sup> yr<sup>-1</sup> (4410 kg C ha<sup>-1</sup> yr<sup>-1</sup>)  
482 during the “business as usual” years (2010 and 2011 as well as 2013 and 2014). During the  
483 restoration year the site lost 395 g CO<sub>2</sub>-C m<sup>-2</sup> (3950 kg C ha<sup>-1</sup>) (Table 2). Carbon losses (and/or  
484 gains) from methane were < 1 g CH<sub>4</sub>-C m<sup>-2</sup> during all five years.

485 Carbon was gained in both parcels during the pre-ploughing years (Table 4). Considerable net  
486 losses of carbon were calculated for the ploughing year. In contrast, the post-ploughing years  
487 were again recognized as years with large net gains in carbon. Over the observation period of  
488 5 years, the Chamau grassland gained approximately 4 t C ha<sup>-1</sup>, excluding losses via leaching  
489 and deposition of C in form of dust.

490

491

492

493

494

495

496

497

498

499

500

501

502

503

504

## 505 **4 Discussion**

506 The five-year measurement period is representative for other similarly managed grassland  
507 ecosystems in Switzerland. Climate conditions were similar to the long-term average as  
508 described in Wolf et al. (2013). Management activities, such as harvests and subsequent  
509 fertilizer applications, were driven by overall weather conditions, (i.e. 2013 late spring, Figure  
510 2a and b).

511

### 512 *4.1 Technical and methodological aspects of the study*

513 Different techniques are currently applied to measure GHG fluxes from a variety of ecosystems  
514 (Denmead, 2008), each having its advantages and disadvantages or being chosen for a specific  
515 purpose or reason. A common approach to study individual processes or time periods  
516 contributing to specific greenhouse gas emissions is to measure with GHG chambers on the  
517 plot scale (Pavelka et al., 2018). Chamber methods have been widely used to derive annual  
518 GHG and nutrient budgets (Barton et al., 2015; Butterbach-Bahl et al., 2013). Critical  
519 assessments of the suitability and associated uncertainty in chamber derived GHG budgets in  
520 relation to sampling frequency have been published by Barton et al. (2013). Existing studies  
521 have not only compared the two measurement techniques employed in this study (manual  
522 chambers and eddy covariance) in grasslands before, but also estimated annual emissions based  
523 on differing methodologies (Flechard et al., 2007; Jones et al., 2017). Additional confidence in  
524 our approach was obtained from the N<sub>2</sub>O emissions during the summer period 2013, where  
525 both measurement techniques ran in parallel (Figure 3a and b). Annual budgets derived by  
526 applying similar gap-filling approaches to the individual datasets led to comparable results  
527 (Table 2).

528 We calculated detection limits for the individual GHGs from our manual chambers following  
529 (Parkin et al., 2012). Detection limits were  $0.34 \pm 0.26 \text{ nmol m}^{-2} \text{ s}^{-1}$ ,  $0.05 \pm 0.02 \text{ nmol m}^{-2} \text{ s}^{-1}$ ,  
530 and  $0.06 \pm 0.06 \text{ } \mu\text{mol m}^{-2} \text{ s}^{-1}$  for CH<sub>4</sub>, N<sub>2</sub>O and CO<sub>2</sub>, respectively. Following this, methane flux  
531 measurements frequently were below this limit of detection, hence we did not calculate  
532 methane budgets for 2010 and 2011. The flux values measured with the EC technique between  
533 2012 and 2014 compare well to similar measurements made by Felber et al. (2016) in an  
534 intensively managed grassland in Western Switzerland. The observed values have been  
535 identified to represent the soil methane exchange in EC measured fluxes (Felber et al. 2016).  
536 N<sub>2</sub>O fluxes in contrast were much better constrained by both methods due to clear N<sub>2</sub>O sources  
537 (i.e. fertilizer amendments) and better sensitivity of the instruments used by both techniques



538 for N<sub>2</sub>O as compared to CH<sub>4</sub>. Background N<sub>2</sub>O emissions as observed in this study ( $0.21 \pm$   
539  $0.55 \text{ nmol m}^{-2} \text{ s}^{-1}$  (SE = 0.02)) compare well to estimates suggested by Rafique et al., (2011)  
540 whom suggest an annual background N<sub>2</sub>O losses of 1.8 kg N<sub>2</sub>O-N for a grazed pasture (i.e.  
541  $0.20 \text{ nmol m}^{-2} \text{ s}^{-1}$ ).

542

#### 543 *4.2 Annual GHG and C and N gains/losses*

544 Net carbon losses and gains estimated for the CH-Cha site between 2010 and 2015 were in  
545 general within the range of values estimated by Zeeman et al., (2010) for the years 2006 and  
546 2007. The slightly higher losses observed prior to ploughing may result from reduced  
547 productivity of the sward. This becomes particularly visible when compared to the net  
548 ecosystem exchange (NEE) of CO<sub>2</sub> values for the years after restoration. Losses via leaching  
549 have previously been estimated to be of minor importance at this site (Zeeman et al., 2010) and  
550 were therefore not considered in this study. Considerably higher C gains during post-ploughing  
551 years were caused by enhanced plant growth in spring and summer. Restoration is primarily  
552 done to eradicate weeds and rodents, favouring biomass productivity of the fodder grass  
553 composition. Other grasslands in Central Europe, i.e. sites in Austria, France and Germany,  
554 showed similar values for net ecosystem exchange (Hörtnagl et al., 2018). Still, total C budgets  
555 as presented here are subject to considerable uncertainty which is strongly depending on  
556 assumptions made for gap-filling etc. (Foken et al., 2004). Nevertheless, the values reported  
557 here show the overall trend on C uptake/release of the site and clearly exceed the uncertainty  
558 of  $\pm 50 \text{ g C per year}$  for eddy covariance studies as suggested by Baldocchi (2003).

559 Methane was of negligible importance for the C budget of this site. We did not observe distinct  
560 peaks in CH<sub>4</sub> emissions in relation to grazing which is primarily due to the low grazing pressure  
561 at CH-Cha. Studies carried out on pastures in Scotland, Mongolia, France and Western  
562 Switzerland have shown that grazing can largely contribute to ecosystem-scale methane fluxes,  
563 in particular if ruminants such as cattle are populating the EC footprint (Dengel et al., 2011;  
564 Felber et al., 2015; Schönbach et al., 2012). If we included an approximation of methane  
565 emissions of cattle which we may have missed in the EC flux measurements, we would have  
566 to add  $3.67 \text{ g CH}_4\text{-C m}^{-2} \text{ y}^{-1}$  to the current value of  $1.48 \text{ g CH}_4\text{-C m}^{-2}$  in 2014 (Table 2). This  
567 value is based on the average methane emissions of  $404 \text{ g CH}_4 \text{ head}^{-1} \text{ d}^{-1}$  stated in Felber et al.  
568 (2016) and linking this to the average stocking density ( $4.04 \text{ head ha}^{-1}$ ) on the Chamua site  
569 and the stocking duration (30 days in 2014). Still, the GHG budget as well as the C budget of  
570 the site would not be altered.

571 The nitrous oxide budget reported for the years without ploughing in this study coincides with  
572 values reported for other grasslands in Europe, ranging from moist to dry climates and lower  
573 to higher elevations in Austria and Switzerland (Cowan et al., 2016; Hörtnagl et al., 2018; Imer  
574 et al., 2013; Skiba et al., 2013).

575 Nitrogen inputs and losses via N<sub>2</sub>O varied largely between the years before and after ploughing.  
576 While the site was characterized by large N amendments prior to ploughing and with reduced  
577 harvest, the picture was completely the opposite during the years after ploughing, with  
578 considerably less N inputs compared to the nitrogen removed from the field via harvests.  
579 Farmers aim every year at having a balanced N budget (fertilizer inputs = nutrients removed  
580 from the field). Pasture degradation is the main motivation for enhanced fertilizer inputs in  
581 order to stabilize forage productivity. Similarly, regular restoration of permanent pastures is  
582 absolutely necessary (Cowan et al., 2016). So far, we identified only one study that investigated  
583 the net effects on the overall GHG exchange following grassland restoration (Drewer et al.,  
584 2017).

585

## 586 **5 Conclusion**

587 This study in combination with an overview of available datasets on grassland restoration and  
588 their consequences on GHG budgets highlights the overall need of additional observational  
589 data. While restoration changed the previous C sink to a C source at the Chamau site, the wider  
590 implication in terms of the GWP of the site when including other GHGs have long-term  
591 consequences (i.e. in mitigation assessments). Furthermore, this study showed the large  
592 variations in N inputs and N outputs from this grassland and the difficulty farmers face when  
593 aiming for balanced N budgets in the field. Still, the current study focused on GHGs only and  
594 can thus not constrain the N budget but assess the losses of N via N<sub>2</sub>O. Losses in form of NH<sub>3</sub>,  
595 N<sub>2</sub> and NO<sub>x</sub> will have to be quantified to fully assess N budgets besides the overall fact that  
596 GHG data following grassland restoration remain largely limited to investigate long-term  
597 consequences. Fortunately, these are likely to become available in the near future by the  
598 establishment of environmental research infrastructures (i.e. ICOS in Europe, NEON in the  
599 USA or TERN in Australia) that aim at standardized, high quality and high temporal resolution  
600 trace gas observation of major ecosystems, including permanent grasslands. With these  
601 additional data, another major constraint of producing defensible GHG and nutrient budgets,  
602 namely gap-filling procedures, will likely be overcome. New and existing data can be used to  
603 derive reliable functional relations and artificial neural networks (ANNs) at field to ecosystem

604 scale that are capable of reproducing in-situ measured data. Once this step is achieved, both  
605 the available data as well the functional relations can be used to improve, to train and to validate  
606 existing biogeochemical process models (Fuchs et al., 2020). Subsequently, reliable  
607 projections on both nutrient and GHG budgets at the ecosystem scale that are driven by  
608 anthropogenic management as well as climatic variability become reality.

609 The study stresses the necessity of including management activities occurring at low frequency  
610 such as ploughing in GHG and nutrient budget estimates. Only then, the effect of potential  
611 best-bet climate change mitigation options can be thoroughly quantified. The next steps in  
612 GHG observations from grassland must not only focus on observing business as usual  
613 activities, but also aim at testing the just mentioned best-bet mitigation options jointly in the  
614 field while simultaneously in combination with existing biogeochemical process models.

615

616

617

618

## 619 **6 Tables and Figures**

620

621 **Table 1:** Table 1: Data availability of GHG fluxes measured over the five-year observation  
622 period. Values are given as all data possible, raw processed values and high quality (HQ) data  
623 or for the chamber flux data if above the detection limit, which were then used in the analysis.  
624 Grey shaded areas represent time period where both methods (EC and static chambers) were  
625 used simultaneously to estimate  $F_{N_2O}$ . Static chamber flux data are further marked in *italic* font.

626

627 **Table 2:** Annual average  $CO_2$ ,  $CH_4$  and  $N_2O$  fluxes and annual sums for the three GHGs as  
628 well as carbon and nitrogen gain/losses per gas species. GWP were calculated for a 100-year  
629 time horizon and based on the most recent numbers provided by IPCC (Stocker et al., 2013).  
630 Annual budgets were derived from either gap-filled manual chamber (MC) or eddy covariance  
631 (EC) measurements. n.c. stands for not calculated. Numbers in *italic* for  $N_2O$  in the years  
632 2010/2011 are likely incomplete due to limited data availability. Sign convention: positive  
633 values denote export/release, negative values import/uptake.

634

635 **Table 3:** Average GHG flux rates per season: winter (DJF), spring (MAM), summer (JJA) and  
636 fall (SON). Values are based on gap-filled data to avoid bias from missing nighttime data  
637 (predominantly relevant for  $CO_2$ ). Data are only presented when continuous measurements  
638 (eddy covariance data) were available. Sign convention: positive values denote export/release,  
639 negative values import/uptake.

640

641 **Table 4:** Table 4: Carbon and nitrogen gains/losses through fertilization, harvest and GHGs  
642 for the Chamau (CH-Cha) site in 2010- 2014. Values are given in  $kg\ ha^{-1}$ . Gains are indicated  
643 with "-" and losses/exports are indicated with "+". While management information was

644 available for both parcels (A and B), flux measurements are an integrate of both parcels. n.c. =  
645 not calculated

646

647 **Table 5:** Existing studies investigating the GHG exchange over pastures following ploughing.  
648 Results presented show the flux magnitude following ploughing and are rounded values of the  
649 individual presented in the papers. Values were converted to similar units ( $\text{mg CO}_2\text{-C m}^{-2} \text{ h}^{-1}$ ,  
650  $\mu\text{g CH}_4\text{-C m}^{-2} \text{ h}^{-1}$  and  $\mu\text{g N}_2\text{O-N m}^{-2} \text{ h}^{-1}$ ). Based on Web of Knowledge search July 15th 2017  
651 with the search terms "grassland", "pasture", "greenhouse gas", "ploughing" and/or "tillage".  
652 Only two studies representing conversion from pasture to cropland or other systems were  
653 included in this table.

654

655 **Table S1:** Detailed management information for the two parcels under investigation at the  
656 Chamau research station. Data are based on fieldbooks provided by the farm personnel as well  
657 as in-situ measurements. Organic fertilizer samples were sent to a central laboratory for nutrient  
658 content analysis (Labor fuer Boden- und Umweltanalytik, Eric Schweizer AG, Thun,  
659 Switzerland). Destructive harvests ( $n = 10$ ) of biomass were carried out in the years 2010, 2011,  
660 2013 and 2014. Harvest estimates are based on values derived from the in-situ measurements  
661 and data provided by the farm personnel. Detailed information on the grazing regime was  
662 furthermore provided by the farm personnel in hand-written form (not shown).

663

664 **Figure 1:** Weather conditions during the years 2010 – 2014. Weather data were measured with  
665 our meteorological sensors installed on site. (a) Daily sum of precipitation (mm) and soil water  
666 content (SWC, blue line,  $\text{m}^3 \text{ m}^{-3}$ ) measured at 5 cm soil depth; (b) daily averaged air  
667 temperature ( $^{\circ}\text{C}$ ), daily averaged soil temperature (grey line,  $^{\circ}\text{C}$ ) and days with snow cover  
668 (horizontal bars); (c) daily averaged photosynthetic photon flux density (PPFD,  $\mu\text{mol m}^{-2} \text{ s}^{-1}$ ).  
669 Days with snow cover were identified with albedo calculations. Days with albedo  $> 0.45$  were  
670 identified as days with either snow or hoarfrost cover.

671

672 **Figure 2:** Management activities for both parcels (A and B in panels (a) and (b), respectively)  
673 on the CH-Cha site. Overall management varied particularly in 2010 between both parcels,  
674 whereas similar management took place between 2011 and 2014. Arrow direction indicates  
675 whether carbon (C in  $\text{kg ha}^{-1}$ ) and/or nitrogen (N in  $\text{kg ha}^{-1}$ ) were amended to, or exported from  
676 the site ("F<sub>o</sub>" and "F<sub>o\*</sub>" - organic fertilizers, slurry/manure (red); "F<sub>m</sub>" - mineral fertilizer (light  
677 orange); "H" - harvest (light blue); "G<sub>s</sub>" and "G<sub>c</sub>" - grazing with sheep/cows (light/dark  
678 brown). Other colored arrows visualize any other management activities such as pesticide  
679 application ("P<sub>h</sub>" - herbicide (light pink); "P<sub>m</sub>" - molluscicide (dark pink); "T" - tillage (black),  
680 "R" - rolling (light grey) and "S" - sowing (dark grey) which occurred predominantly in 2010  
681 (parcel B) and 2012 (parcels A and B). Carbon imports and exports are indicated by black and  
682 grey bars. Thereby black indicated the start of the specific management activities and grey the  
683 duration (e.g. during grazing, "G<sub>s</sub>"). Green colors indicate nitrogen amendments or losses, with  
684 dark green visualizing the start of the activity and light green colors indicating the duration.  
685 Sign convention: positive values denote export/release, negative values import/uptake.

686

687 **Figure 3:** (a) Temporal dynamics of N<sub>2</sub>O fluxes measured with the eddy covariance (white  
688 circles) and manual greenhouse gas chambers (black circles measured in 2013) – grey lines  
689 indicate standard deviation. Arrows indicate management events ("H" = harvest, "F<sub>o</sub>" =  
690 organic fertilizer application (slurry), "Ph" = pesticide (herbicide) application). (b) 1:1  
691 comparison between chamber based and eddy covariance based N<sub>2</sub>O fluxes in 2013. The  
692 dashed line represents the 1:1 line. ( $y = mx + c$ ,  $r^2 = 0.4$ ,  $m = 0.61$ ,  $c = 0.17$ ,  $p < 0.0001$ ). Sign  
693 convention: positive values denote export/release, negative values import/uptake.

694  
695  
696  
697  
698  
699  
700  
701  
702  
703  
704  
705  
706  
707  
708  
709  
710  
711  
712  
713  
714  
715  
716  
717  
718  
719  
720  
721  
722  
723  
724  
725  
726  
727  
728  
729  
730

**Figure 4:** Temporal dynamics of gap-filled (except methane in 2010/2011) daily averaged greenhouse gas (GHG) fluxes (white circles): a) (CO<sub>2</sub> exchange in  $\mu\text{mol m}^{-2} \text{s}^{-1}$ ); (b) CH<sub>4</sub> exchange in  $\text{nmol m}^{-2} \text{s}^{-1}$  and (c) N<sub>2</sub>O exchange in  $\text{nmol m}^{-2} \text{s}^{-1}$ . Coloured circles indicate manual chamber measurements. While both GHGs, CH<sub>4</sub> and N<sub>2</sub>O were measured in 2010 and 2011 (blue circles), N<sub>2</sub>O only was measured in 2013 (light blue circles). The grey dashed lines indicate the beginning of a new year. Same color coding as used in Figure 3 a was used to highlight management activities. Sign convention: positive values denote export/release, negative values import/uptake. Grey lines behind the circles indicate standard deviation.

## 731 **7 Acknowledgements**

732 Funding for this study is gratefully acknowledged and was provided by the following projects:  
733 Models4Pastures (FACCE-JPI project, SNSF funded contract: 40FA40\_154245 / 1), GHG-  
734 Europe (FP7, EU contract No. 244122), COST-ES0804 ABBA and SNF-R'EQUIP  
735 (206021\_133763). We are specifically thankful to Hans-Rudolf Wettstein, Ivo Widmer and  
736 Tina Stiefel for providing crucial management data and support in the field. Further, this project  
737 could not have been accomplished without the help from the technical team, specifically Peter  
738 Plüss, Thomas Baur, Florian Käslin, Philip Meier and Patrick Flütsch. We greatly acknowledge  
739 their help during the planning stage, and the endurance during the setup of the new QCLAS  
740 system as well as regular trouble shooting of the Swissfluxnet Chamau (CH-Cha) research site.

741

742

## 743 **8 Author contributions**

744 LM and LH designed the study and wrote the first manuscript version. LM, CD, WE KF and  
745 BW collected the data in the field. LH further provided the code for flux processing. All authors  
746 revised and commented on the manuscript.

747

## 748 **9 Data availability**

749 All flux and meta data are openly available via Fluxnet. The flux processing code is available  
750 via the Grassland Sciences Group at ETH Zurich. Greenhouse gas chamber data are available  
751 via Imer et al. 2013.

752

753

754

755

756

757

758

759

760

761

762

763

764 **10 References**

765

766 Ambus, P., Clayton, H., Arah, J. R. M., Smith, K. A. and Christensen, S.: Similar N<sub>2</sub>O flux  
767 from soil measured with different chamber techniques, *Atmos. Environ. Part A, Gen. Top.*,  
768 doi:10.1016/0960-1686(93)90078-D, 1993.

769

770 Ammann, C., Neftel, A., Jocher, M., Fuhrer, J. and Leifeld, J.: Effect of management and  
771 weather variations on the greenhouse gas budget of two grasslands during a 10-year  
772 experiment, *Agriculture, Ecosystems & Environment*, 292, 106814,  
773 doi:https://doi.org/10.1016/j.agee.2019.106814, 2020.

774

775 Baldocchi, D. D.: Assessing the eddy covariance technique for evaluating carbon dioxide  
776 exchange rates of ecosystems: Past, present and future, *Glob. Chang. Biol.*, doi:10.1046/j.1365-  
777 2486.2003.00629.x, 2003.

778

779 Baldocchi, D., Detto, M., Sonnentag, O., Verfaillie, J., Teh, Y. A., Silver, W. and Kelly, N.  
780 M.: The challenges of measuring methane fluxes and concentrations over a peatland pasture,  
781 *Agric. For. Meteorol.*, doi:10.1016/j.agrformet.2011.04.013, 2012.

782

783 Baldocchi, D.: Measuring fluxes of trace gases and energy between ecosystems and the  
784 atmosphere - the state and future of the eddy covariance method, *Glob. Chang. Biol.*,  
785 doi:10.1111/gcb.12649, 2014.

786

787 Ball, B. C., Scott, A. and Parker, J. P.: Field N<sub>2</sub>O, CO<sub>2</sub> and CH<sub>4</sub> fluxes in relation to tillage,  
788 compaction and soil quality in Scotland, *Soil Tillage Res.*, doi:10.1016/S0167-1987(99)00074-  
789 4, 1999.

790

791 Barton, L., Wolf, B., Rowlings, D., Scheer, C., Kiese, R., Grace, P., Stefanova, K. and  
792 Butterbach-Bahl, K.: Sampling frequency affects estimates of annual nitrous oxide fluxes, *Sci.*  
793 *Rep.*, doi:10.1038/srep15912, 2015.

794

795 Beyer, C., Liebersbach, H. and Höper, H.: Multiyear greenhouse gas flux measurements on a  
796 temperate fen soil used for cropland or grassland, *J. Plant Nutr. Soil Sci.*,  
797 doi:10.1002/jpln.201300396, 2015.

798

799 Brümmer, C., Lyshede, B., Lempio, D., Delorme, J. P., Ruffer, J. J., Fuß, R., Moffat, A. M.,  
800 Hurkuck, M., Ibrom, A., Ambus, P., Flessa, H. and Kutsch, W. L.: Gas chromatography vs.  
801 quantum cascade laser-based N<sub>2</sub>O flux measurements using a novel chamber design,  
802 *Biogeosciences*, doi:10.5194/bg-14-1365-2017, 2017.

803

804 Buchen, C., Well, R., Helfrich, M., Fuß, R., Kayser, M., Gensior, A., Benke, M. and Flessa,  
805 H.: Soil mineral N dynamics and N<sub>2</sub>O emissions following grassland renewal, *Agric. Ecosyst.*  
806 *Environ.*, doi:10.1016/j.agee.2017.06.013, 2017.

807

808 Butterbach-Bahl, K., Kiese, R. and Liu, C.: Measurements of biosphere atmosphere exchange  
809 of CH<sub>4</sub> in terrestrial ecosystems, in *Methods in Enzymology.*, 2011.

810

811 Butterbach-Bahl, K., Baggs, E. M., Dannenmann, M., Kiese, R. and Zechmeister-Boltenstern,  
812 S.: Nitrous oxide emissions from soils: How well do we understand the processes and their  
813 controls?, *Philos. Trans. R. Soc. B Biol. Sci.*, doi:10.1098/rstb.2013.0122, 2013.  
814

815 Chiavegato, M. B., Powers, W. J., Carmichael, D. and Rowntree, J. E.: Pasture-derived  
816 greenhouse gas emissions in cow-calf production systems, *J. Anim. Sci.*, doi:10.2527/jas.2014-  
817 8134, 2015.  
818

819 Chen, Z., Ding, W., Xu, Y., Müller, C., Yu, H. and Fan, J.: Increased N<sub>2</sub>O emissions during  
820 soil drying after waterlogging and spring thaw in a record wet year, *Soil Biol. Biochem.*,  
821 doi:10.1016/j.soilbio.2016.07.016, 2016.  
822

823 Ciais, P., Reichstein, M., Viovy, N., Granier, A., Ogée, J., Allard, V., Aubinet, M., Buchmann,  
824 N., Bernhofer, C., Carrara, A., Chevallier, F., De Noblet, N., Friend, A. D., Friedlingstein, P.,  
825 Grünwald, T., Heinesch, B., Keronen, P., Knohl, A., Krinner, G., Loustau, D., Manca, G.,  
826 Matteucci, G., Miglietta, F., Ourcival, J. M., Papale, D., Pilegaard, K., Rambal, S., Seufert, G.,  
827 Soussana, J. F., Sanz, M. J., Schulze, E. D., Vesala, T. and Valentini, R.: Europe-wide reduction  
828 in primary productivity caused by the heat and drought in 2003, *Nature*,  
829 doi:10.1038/nature03972, 2005.  
830

831 Cowan, N. J., Levy, P. E., Famulari, D., Anderson, M., Drewer, J., Carozzi, M., Reay, D. S.  
832 and Skiba, U. M.: The influence of tillage on N<sub>2</sub>O fluxes from an intensively managed grazed  
833 grassland in Scotland, *Biogeosciences*, doi:10.5194/bg-13-4811-2016, 2016.  
834

835 Denmead, O. T.: Approaches to measuring fluxes of methane and nitrous oxide between  
836 landscapes and the atmosphere, *Plant Soil*, doi:10.1007/s11104-008-9599-z, 2008.  
837

838 Drewer, J., Anderson, M., Levy, P. E., Scholtes, B., Helfter, C., Parker, J., Rees, R. M. and  
839 Skiba, U. M.: The impact of ploughing intensively managed temperate grasslands on N<sub>2</sub>O,  
840 CH<sub>4</sub> and CO<sub>2</sub> fluxes, *Plant Soil*, doi:10.1007/s11104-016-3023-x, 2017.  
841

842 Eugster, W. and Plüss, P.: A fault-tolerant eddy covariance system for measuring CH<sub>4</sub> fluxes,  
843 *Agric. For. Meteorol.*, doi:10.1016/j.agrformet.2009.12.008, 2010.  
844

845 Eugster, W. and Merbold, L.: Eddy covariance for quantifying trace gas fluxes from soils,  
846 *SOIL*, doi:10.5194/soil-1-187-2015, 2015.  
847

848 Felber, R., Münger, A., Neftel, A. and Ammann, C.: Eddy covariance methane flux  
849 measurements over a grazed pasture: Effect of cows as moving point sources, *Biogeosciences*,  
850 doi:10.5194/bg-12-3925-2015, 2015.  
851

852 Flechard, C. R., Ambus, P., Skiba, U., Rees, R. M., Hensen, A., van Amstel, A., Dasselaar, A.  
853 van den P. van, Soussana, J. F., Jones, M., Clifton-Brown, J., Raschi, A., Horvath, L., Neftel,  
854 A., Jocher, M., Ammann, C., Leifeld, J., Fuhrer, J., Calanca, P., Thalman, E., Pilegaard, K., Di  
855 Marco, C., Campbell, C., Nemitz, E., Hargreaves, K. J., Levy, P. E., Ball, B. C., Jones, S. K.,  
856 van de Bulk, W. C. M., Groot, T., Blom, M., Domingues, R., Kasper, G., Allard, V., Ceschia,  
857 E., Cellier, P., Laville, P., Henault, C., Bizouard, F., Abdalla, M., Williams, M., Baronti, S.,  
858 Berretti, F. and Grosz, B.: Effects of climate and management intensity on nitrous oxide  
859 emissions in grassland systems across Europe, *Agric. Ecosyst. Environ.*,  
860 doi:10.1016/j.agee.2006.12.024, 2007.



861  
862 Foken, T., Gockede, M., Mauder, M., Mahrt, L., Amiro, B. and Munger, W.: Handbook of  
863 Micrometeorology: A Guide for surface flux measurement and analysis: Chapter 9: POST-  
864 FIELD DATA QUALITY CONTROL., 2004.  
865  
866 Foken, T., Göckede, M., Mauder, M., Mahrt, L., Amiro, B. and Munger, W.: Post-Field Data  
867 Quality Control, in Handbook of Micrometeorology., 2006.  
868  
869 Fratini, G., McDermitt, D. K. and Papale, D.: Eddy-covariance flux errors due to biases in gas  
870 concentration measurements: Origins, quantification and correction, Biogeosciences,  
871 doi:10.5194/bg-11-1037-2014, 2014.  
872  
873 Fratini, G. and Mauder, M.: Towards a consistent eddy-covariance processing: An  
874 intercomparison of EddyPro and TK3, Atmos. Meas. Tech., doi:10.5194/amt-7-2273-2014,  
875 2014.  
876  
877 Fuchs, K., Hörtnagl, L., Buchmann, N., Eugster, W., Snow, V. and Merbold, L.: Management  
878 matters: Testing a mitigation strategy for nitrous oxide emissions using legumes on intensively  
879 managed grassland, Biogeosciences, doi:10.5194/bg-15-5519-2018, 2018.  
880  
881 Fuchs, K., Merbold, L., Buchmann, N., Bretscher, D., Brilli, L., Fitton, N., Topp, C. F. E.,  
882 Klumpp, K., Lieffering, M., Martin, R., Newton, P. C. D., Rees, R. M., Rolinski, S., Smith, P.  
883 and Snow, V.: Multimodel Evaluation of Nitrous Oxide Emissions From an Intensively  
884 Managed Grassland, J. Geophys. Res. Biogeosciences, 125(1), 1–21,  
885 doi:10.1029/2019JG005261, 2020.  
886  
887 Dengel, S., Levy, P. E., Grace, J., Jones, S. K. and Skiba, U. M.: Methane emissions from  
888 sheep pasture, measured with an open-path eddy covariance system, Glob. Chang. Biol.,  
889 doi:10.1111/j.1365-2486.2011.02466.x, 2011.  
890  
891 Hartmann, A. A. and Niklaus, P. A.: Effects of simulated drought and nitrogen fertilizer on  
892 plant productivity and nitrous oxide (N<sub>2</sub>O) emissions of two pastures, Plant Soil,  
893 doi:10.1007/s11104-012-1248-x, 2012.  
894  
895 Hopkins, A. and Del Prado, A.: Implications of climate change for grassland in Europe:  
896 Impacts, adaptations and mitigation options: A review, Grass Forage Sci., doi:10.1111/j.1365-  
897 2494.2007.00575.x, 2007.  
898  
899 Hörtnagl, L. and Wohlfahrt, G.: Methane and nitrous oxide exchange over a managed hay  
900 meadow, Biogeosciences, doi:10.5194/bg-11-7219-2014, 2014.  
901  
902 Hörtnagl, L., Barthel, M., Buchmann, N., Eugster, W., Butterbach-Bahl, K., Díaz-Pinés, E.,  
903 Zeeman, M., Klumpp, K., Kiese, R., Bahn, M., Hammerle, A., Lu, H., Ladreiter-Knauss, T.,  
904 Burri, S. and Merbold, L.: Greenhouse gas fluxes over managed grasslands in Central Europe,  
905 Glob. Chang. Biol., doi:10.1111/gcb.14079, 2018.  
906  
907 Imer, D., Merbold, L., Eugster, W. and Buchmann, N.: Temporal and spatial variations of soil  
908 CO<sub>2</sub>, CH<sub>4</sub> and N<sub>2</sub>O fluxes at three differently managed grasslands, Biogeosciences,  
909 doi:10.5194/bg-10-5931-2013, 2013.  
910

911 Jones, S. K., Helfter, C., Anderson, M., Coyle, M., Campbell, C., Famulari, D., Di Marco, C.,  
912 Van Dijk, N., Sim Tang, Y., Topp, C. F. E., Kiese, R., Kindler, R., Siemens, J., Schrumpf, M.,  
913 Kaiser, K., Nemitz, E., Levy, P. E., Rees, R. M., Sutton, M. A. and Skiba, U. M.: The nitrogen,  
914 carbon and greenhouse gas budget of a grazed, cut and fertilised temperate grassland,  
915 *Biogeosciences*, doi:10.5194/bg-14-2069-2017, 2017.  
916  
917 Kim, Y. and Tanaka, N.: Fluxes of CO<sub>2</sub>, N<sub>2</sub>O and CH<sub>4</sub> by <sup>222</sup>Rn and chamber methods in  
918 cold-temperate grassland soil, northern Japan, *Soil Sci. Plant Nutr.*,  
919 doi:10.1080/00380768.2014.967167, 2015.  
920  
921 Knox, S. H., Sturtevant, C., Matthes, J. H., Koteen, L., Verfaillie, J. and Baldocchi, D.:  
922 Agricultural peatland restoration: Effects of land-use change on greenhouse gas (CO<sub>2</sub> and  
923 CH<sub>4</sub>) fluxes in the Sacramento-San Joaquin Delta, *Glob. Chang. Biol.*, doi:10.1111/gcb.12745,  
924 2015.  
925  
926 Krol, D. J., Jones, M. B., Williams, M., Richards, K. G., Bourdin, F. and Lanigan, G. J.: The  
927 effect of renovation of long-term temperate grassland on N<sub>2</sub>O emissions and N leaching from  
928 contrasting soils, *Sci. Total Environ.*, doi:10.1016/j.scitotenv.2016.04.052, 2016.  
929  
930 Kroon, P. S., Hensen, A., Jonker, H. J. J., Zahniser, M. S., Van't Veen, W. H. and Vermeiden,  
931 A. T.: Suitability of quantum cascade laser spectroscopy for CH<sub>4</sub> and N<sub>2</sub>O eddy covariance  
932 flux measurements, *Biogeosciences*, doi:10.5194/bg-4-715-2007, 2007.  
933  
934 Kroon, P. S., Vesala, T. and Grace, J.: Flux measurements of CH<sub>4</sub> and N<sub>2</sub>O exchanges, *Agric.*  
935 *For. Meteorol.*, doi:10.1016/j.agrformet.2009.11.017, 2010.  
936  
937 Lal, R.: Soil carbon sequestration impacts on global climate change and food security, *Science*  
938 (80-. ), doi:10.1126/science.1097396, 2004.  
939  
940 Laubach, J., Barthel, M., Fraser, A., Hunt, J. E. and Griffith, D. W. T.: Combining two  
941 complementary micrometeorological methods to measure CH<sub>4</sub> and N<sub>2</sub>O fluxes over pasture,  
942 *Biogeosciences*, doi:10.5194/bg-13-1309-2016, 2016.  
943  
944 Lundegardh, H.: Carbon dioxide evolution of soil and crop growth, *Soil Sci.*,  
945 doi:10.1097/00010694-192706000-00001, 1927.  
946  
947 MacDonald, J. D., Rochette, P., Chantigny, M. H., Angers, D. A., Royer, I. and Gasser, M. O.:  
948 Ploughing a poorly drained grassland reduced N<sub>2</sub>O emissions compared to chemical fallow,  
949 *Soil Tillage Res.*, doi:10.1016/j.still.2010.09.005, 2011.  
950  
951 MacKenzie, A. F., Fan, M. X. and Cadrin, F.: Nitrous oxide emission as affected by tillage,  
952 corn-soybean-alfalfa rotations and nitrogen fertilization, in *Canadian Journal of Soil Science.*,  
953 1997.  
954  
955 Matzner, E. and Borken, W.: Do freeze-thaw events enhance C and N losses from soils of  
956 different ecosystems? A review, *Eur. J. Soil Sci.*, doi:10.1111/j.1365-2389.2007.00992.x,  
957 2008.  
958

959 Merbold, L., Eugster, W., Stieger, J., Zahniser, M., Nelson, D. and Buchmann, N.: Greenhouse  
960 gas budget (CO<sub>2</sub>, CH<sub>4</sub> and N<sub>2</sub>O) of intensively managed grassland following restoration,  
961 *Glob. Chang. Biol.*, doi:10.1111/gcb.12518, 2014.

962

963 Mishurov, M. and Kiely, G.: Gap-filling techniques for the annual sums of nitrous oxide fluxes,  
964 *Agric. For. Meteorol.*, doi:10.1016/j.agrformet.2011.07.014, 2011.

965

966 Moffat, A. M., Papale, D., Reichstein, M., Hollinger, D. Y., Richardson, A. D., Barr, A. G.,  
967 Beckstein, C., Braswell, B. H., Churkina, G., Desai, A. R., Falge, E., Gove, J. H., Heimann,  
968 M., Hui, D., Jarvis, A. J., Kattge, J., Noormets, A. and Stauch, V. J.: Comprehensive  
969 comparison of gap-filling techniques for eddy covariance net carbon fluxes, *Agric. For.*  
970 *Meteorol.*, doi:10.1016/j.agrformet.2007.08.011, 2007.

971

972 Mudge, P. L., Wallace, D. F., Rutledge, S., Campbell, D. I., Schipper, L. A. and Hosking, C.  
973 L.: Carbon balance of an intensively grazed temperate pasture in two climatically: Contrasting  
974 years, *Agric. Ecosyst. Environ.*, doi:10.1016/j.agee.2011.09.003, 2011.

975

976 Necpálová, M., Casey, I. and Humphreys, J.: Effect of ploughing and reseeded of permanent  
977 grassland on soil N, N leaching and nitrous oxide emissions from a clay-loam soil, *Nutr. Cycl.*  
978 *Agroecosystems*, doi:10.1007/s10705-013-9564-y, 2013.

979

980 Nemitz, E., Mammarella, I., Ibrom, A., Aurela, M., Burba, G. G., Dengel, S., Gielen, B., Grelle,  
981 A., Heinesch, B., Herbst, M., Hörtnagl, L., Klemetsson, L., Lindroth, A., Lohila, A.,  
982 McDermitt, D. K., Meier, P., Merbold, L., Nelson, D., Nicolini, G., Nilsson, M. B., Peltola, O.,  
983 Rinne, J. and Zahniser, M.: Standardisation of eddy-covariance flux measurements of methane  
984 and nitrous oxide, *Int. Agrophysics*, doi:10.1515/intag-2017-0042, 2018.

985

986 Parkin, T. B., Venterea, R. T. and Hargreaves, S. K.: Calculating the Detection Limits of  
987 Chamber-based Soil Greenhouse Gas Flux Measurements, *J. Environ. Qual.*,  
988 doi:10.2134/jeq2011.0394, 2012.

989

990 Pavelka, M., Acosta, M., Kiese, R., Altimir, N., Brümmer, C., Crill, P., Darenova, E., Fuß, R.,  
991 Gielen, B., Graf, A., Klemetsson, L., Lohila, A., Longdoz, B., Lindroth, A., Nilsson, M.,  
992 Jiménez, S. M., Merbold, L., Montagnani, L., Peichl, M., Pihlatie, M., Pumpanen, J., Ortiz, P.  
993 S., Silvennoinen, H., Skiba, U., Vestin, P., Weslien, P., Janous, D. and Kutsch, W.:  
994 Standardisation of chamber technique for CO<sub>2</sub>, N<sub>2</sub>O and CH<sub>4</sub> fluxes measurements from  
995 terrestrial ecosystems, *Int. Agrophysics*, 32(4), 569–587, doi:10.1515/intag-2017-0045, 2018.

996

997 Pumpanen, J., Kolari, P., Ilvesniemi, H., Minkkinen, K., Vesala, T., Niinistö, S., Lohila, A.,  
998 Larmola, T., Morero, M., Pihlatie, M., Janssens, I., Yuste, J. C., Grünzweig, J. M., Reth, S.,  
999 Subke, J. A., Savage, K., Kutsch, W., Østreg, G., Ziegler, W., Anthoni, P., Lindroth, A. and  
1000 Hari, P.: Comparison of different chamber techniques for measuring soil CO<sub>2</sub> efflux, *Agric.*  
1001 *For. Meteorol.*, doi:10.1016/j.agrformet.2003.12.001, 2004.

1002

1003 Rafique, R., Hennessy, D. and Kiely, G.: Nitrous Oxide Emission from Grazed Grassland  
1004 Under Different Management Systems, *Ecosystems*, 14(4), 563–582 [online] Available from:  
1005 <http://www.jstor.org/stable/41505893>, 2011.

1006

1007 Reichstein, M., Falge, E., Baldocchi, D., Papale, D., Aubinet, M., Berbigier, P., Bernhofer, C.,  
1008 Buchmann, N., Gilmanov, T., Granier, A., Grünwald, T., Havránková, K., Ilvesniemi, H.,

1009 Janous, D., Knohl, A., Laurila, T., Lohila, A., Loustau, D., Matteucci, G., Meyers, T., Miglietta,  
1010 F., Ourcival, J. M., Pumpanen, J., Rambal, S., Rotenberg, E., Sanz, M., Tenhunen, J., Seufert,  
1011 G., Vaccari, F., Vesala, T., Yakir, D. and Valentini, R.: On the separation of net ecosystem  
1012 exchange into assimilation and ecosystem respiration: Review and improved algorithm, *Glob.*  
1013 *Chang. Biol.*, doi:10.1111/j.1365-2486.2005.001002.x, 2005.

1014

1015 Rochette, P., Ellert, B., Gregorich, E. G., Desjardins, R. L., Pattey, E., Lessard, R. and Johnson,  
1016 B. G.: Description of a dynamic closed chamber for measuring soil respiration and its  
1017 comparison with other techniques, in *Canadian Journal of Soil Science.*, 1997.

1018

1019 Rutledge, S., Wall, A. M., Mudge, P. L., Troughton, B., Campbell, D. I., Pronger, J., Joshi, C.  
1020 and Schipper, L. A.: The carbon balance of temperate grasslands part II: The impact of pasture  
1021 renewal via direct drilling, *Agriculture, Ecosystems & Environment*, 239, 132–142,  
1022 doi:<https://doi.org/10.1016/j.agee.2017.01.013>, 2017.

1023

1024 Schönbach, P., Wolf, B., Dickhöfer, U., Wiesmeier, M., Chen, W., Wan, H., Gierus, M.,  
1025 Butterbach-Bahl, K., Kögel-Knabner, I., Susenbeth, A., Zheng, X. and Taube, F.: Grazing  
1026 effects on the greenhouse gas balance of a temperate steppe ecosystem, *Nutr. Cycl.*  
1027 *Agroecosystems*, doi:10.1007/s10705-012-9521-1, 2012.

1028

1029 Schulze, E. D., Luysaert, S., Ciais, P., Freibauer, A., Janssens, I. A., Soussana, J. F., Smith,  
1030 P., Grace, J., Levin, I., Thiruchittampalam, B., Heimann, M., Dolman, A. J., Valentini, R.,  
1031 Bousquet, P., Peylin, P., Peters, W., Rödenbeck, C., Etiope, G., Vuichard, N., Wattenbach, M.,  
1032 Nabuurs, G. J., Poussi, Z., Nieschulze, J. and Gash, J. H.: Importance of methane and nitrous  
1033 oxide for Europe’s terrestrial greenhouse-gas balance, *Nat. Geosci.*, doi:10.1038/ngeo686,  
1034 2009.

1035

1036 Skiba, U., Hargreaves, K. J., Beverland, I. J., O’Neill, D. H., Fowler, D. and Moncrieff, J. B.:  
1037 Measurement of field scale N<sub>2</sub>O emission fluxes from a wheat crop using micrometeorological  
1038 techniques, *Plant Soil*, doi:10.1007/BF00011300, 1996.

1039

1040 Skiba, U., Jones, S. K., Drewer, J., Helfter, C., Anderson, M., Dinsmore, K., McKenzie, R.,  
1041 Nemitz, E. and Sutton, M. A.: Comparison of soil greenhouse gas fluxes from extensive and  
1042 intensive grazing in a temperate maritime climate, *Biogeosciences*, doi:10.5194/bg-10-1231-  
1043 2013, 2013.

1044

1045 Smith, P., Martino, D., Cai, Z., Gwary, D., Janzen, H., Kumar, P., McCarl, B., Ogle, S.,  
1046 O’Mara, F., Rice, C., Scholes, B., Sirotenko, O., Howden, M., McAllister, T., Pan, G.,  
1047 Romanenkov, V., Schneider, U., Towprayoon, S., Wattenbach, M. and Smith, J.: Greenhouse  
1048 gas mitigation in agriculture, *Philos. Trans. R. Soc. B Biol. Sci.*, doi:10.1098/rstb.2007.2184,  
1049 2008.

1050

1051 Stocker, T. F., Qin, D., Plattner, G. K., Tignor, M. M. B., Allen, S. K., Boschung, J., Nauels,  
1052 A., Xia, Y., Bex, V. and Midgley, P. M.: Climate change 2013 the physical science basis:  
1053 Working Group I contribution to the fifth assessment report of the intergovernmental panel on  
1054 climate change., 2013.

1055

1056 Teh, Y. A., Silver, W. L., Sonnentag, O., Detto, M., Kelly, M. and Baldocchi, D. D.: Large  
1057 Greenhouse Gas Emissions from a Temperate Peatland Pasture, *Ecosystems*,  
1058 doi:10.1007/s10021-011-9411-4, 2011.

1059  
1060 Vellinga, T. V., van den Pol-van Dasselaar, A. and Kuikman, P. J.: The impact of grassland  
1061 ploughing on CO<sub>2</sub> and N<sub>2</sub>O emissions in the Netherlands, *Nutr. Cycl. Agroecosystems*,  
1062 doi:10.1023/b:fres.0000045981.56547.db, 2004.  
1063  
1064 Vickers, D. and Mahrt, L.: Quality control and flux sampling problems for tower and aircraft  
1065 data, *J. Atmos. Ocean. Technol.*, doi:10.1175/1520-0426, 1997.  
1066  
1067 Webb, E. K., Pearman, G. I. and Leuning, R.: Correction of flux measurements for density  
1068 effects due to heat and water vapour transfer, *Q. J. R. Meteorol. Soc.*,  
1069 doi:10.1002/qj.49710644707, 1980.  
1070  
1071 Wecking, A. R., Wall, A. M., Liáng, L. L., Lindsey, S. B., Luo, J., Campbell, D. I. and  
1072 Schipper, L. A.: Reconciling annual nitrous oxide emissions of an intensively grazed dairy  
1073 pasture determined by eddy covariance and emission factors, *Agriculture, Ecosystems &*  
1074 *Environment*, 287, 106646, doi:https://doi.org/10.1016/j.agee.2019.106646, 2020.  
1075  
1076 Wei, D., Ri, X., Tarchen, T., Wang, Y. and Wang, Y.: Considerable methane uptake by alpine  
1077 grasslands despite the cold climate: In situ measurements on the central Tibetan Plateau, 2008-  
1078 2013, *Glob. Chang. Biol.*, doi:10.1111/gcb.12690, 2015.  
1079  
1080 Wolf, S., Eugster, W., Ammann, C., Häni, M., Zielis, S., Hiller, R., Stieger, J., Imer, D.,  
1081 Merbold, L. and Buchmann, N.: Contrasting response of grassland versus forest carbon and  
1082 water fluxes to spring drought in Switzerland, *Environ. Res. Lett.*, doi:10.1088/1748-  
1083 9326/8/3/035007, 2013.  
1084  
1085 Zeeman, M. J., Hiller, R., Gilgen, A. K., Michna, P., Plüss, P., Buchmann, N. and Eugster, W.:  
1086 Management and climate impacts on net CO<sub>2</sub> fluxes and carbon budgets of three grasslands  
1087 along an elevational gradient in Switzerland, *Agric. For. Meteorol.*,  
1088 doi:10.1016/j.agrformet.2010.01.011, 2010.  
1089  
1090 Zenone, T., Zona, D., Gelfand, I., Gielen, B., Camino-Serrano, M. and Ceulemans, R.: CO<sub>2</sub>  
1091 uptake is offset by CH<sub>4</sub> and N<sub>2</sub>O emissions in a poplar short-rotation coppice, *GCB Bioenergy*,  
1092 doi:10.1111/gcbb.12269, 2016.  
1093  
1094 Zona, D., Janssens, I. A., Gioli, B., Jungkunst, H. F., Serrano, M. C. and Ceulemans, R.: N<sub>2</sub>O  
1095 fluxes of a bio-energy poplar plantation during a two years rotation period, *GCB Bioenergy*,  
1096 doi:10.1111/gcbb.12019, 2013.  
1097  
1098  
1099

Table 1: Data availability of GHG fluxes measured over the five-year observation period. Values are given as all data possible, raw processed values and high quality (HQ) data or for the chamber flux data if above the detection limit, which were then used in the analysis. Grey shaded areas represent time period where both methods (EC and static chambers) were used simultaneously to estimate FN<sub>2</sub>O. Static chamber flux data are further marked in italic font.

Year	F <sub>CO<sub>2</sub></sub>			F <sub>CH<sub>4</sub></sub> *			F <sub>N<sub>2</sub>O</sub> *		
	max data availability	raw fluxes	HQ fluxes (0,1)	max data availability	raw fluxes	HQ fluxes (0,1)	max data availability	raw fluxes	HQ fluxes (0,1)
<b>2010</b>									
<b>30min</b>	17520	16064	10171	365	19	1	365	19	19
<b>%</b>	100	91.68	58.05	100	12.05	0.27	100	12.05	5.21
<b>2011</b>									
<b>30min</b>	17520	14873	10002	365	16	2	365	16	14
<b>%</b>	100	84.8	57.08	100	4.38	0.55	100	4.38	3.84
<b>2012</b>									
<b>30min</b>	17568	15361	10165	17568	15523	10181	17568	15528	12859
<b>%</b>	100	87.43	57.85	100	88.35	57.95	100	88.38	73.19
<b>2013</b>									
<b>30min</b>	17520	14825	10409	17520	17200	11310	17520 (365)	17200 (52)	11790 (39)
<b>%</b>	100	84.61	59.4	100	98.16	64.55	100 (100)	98.16 (14.24)	67.29 (10.68)
<b>2014</b>									
<b>30min</b>	17520	15719	10064	17520	17207	11166	17520	17207	11986
<b>%</b>	100	89.71	57.43	100	98.2	63.72	100	98.2	68.4
<b>All Years</b>									
<b>30min</b>	<b>87648</b>	<b>76842</b>	<b>50811</b>	<b>87548 (1826)</b>	<b>49930 (35)</b>	<b>32657 (3)</b>	<b>87648 (1826)</b>	<b>49935 (112)</b>	<b>36635 (72)</b>
<b>%</b>	<b>100</b>	<b>87.67</b>	<b>57.97</b>	<b>100 (100)</b>	<b>57.03 (1.91)</b>	<b>37.30 (0.16)</b>	<b>100 (100)</b>	<b>57.03 (6.13)</b>	<b>41.94 (3.94)</b>

\* data availability in parenthesis are based on static manual chambers (2010 and 2011, approx. biweekly measurements (n = 19 and 16 respectively, Imer et al. 2013), as well as during summer 2013 (n = 52)). High quality data were only data points that were above the minimum detection limits calculated. For further information see the methodology.

**Table 2:** Annual average CO<sub>2</sub>, CH<sub>4</sub> and N<sub>2</sub>O fluxes and annual sums for the three GHGs as well as carbon and nitrogen gain/losses per gas species. GWP were calculated for a 100-year time horizon and based on the most recent numbers provided by IPCC (Stocker et al., 2013). Annual budgets were derived from either gap-filled manual chamber (MC) or eddy covariance (EC) measurements. n.c. stands for not calculated. Numbers in italic for N<sub>2</sub>O in the years 2010/2011 are likely incomplete due to limited data availability. **Sign convention: positive values denote export/release, negative values import/uptake.**

	2010 (MC)	2010 (EC)	2011 (MC)	2011 (EC)	2012 (MC)	2012 (EC)	2013 (MC)	2013 (EC)	2014 (MC)	2014 (EC)
Average CO <sub>2</sub> flux $\mu\text{mol m}^{-2} \text{ s}^{-1}$		-0.5		-0.7		1.04		-1.4		-1.98
STDEV Average CO <sub>2</sub> flux $\mu\text{mol m}^{-2} \text{ s}^{-1}$		3.11		3.63		3.02		3.52		3.9
g CO <sub>2</sub> m <sup>-2</sup>		-695.23		-978.16		1447.16		-2047.8		-2751.66
g CO <sub>2</sub> -C m <sup>-2</sup>		-189.6		-266.77		394.68		-558.49		-750.45
Global warming potential in g CO <sub>2</sub> -eq. m <sup>-2</sup>		<b>-695.23</b>		<b>-978.16</b>		<b>1447.16</b>		<b>-2047.8</b>		<b>-2751.66</b>
% of the total budget		<b>69.2</b>		<b>91.6</b>		<b>55.1</b>		<b>92.3</b>		<b>94</b>
Average CH <sub>4</sub> flux $\text{nmol m}^{-2} \text{ s}^{-1}$	n.c.		n.c.			1.91		3.67		3.92
STDEV Average CH <sub>4</sub> flux $\text{nmol m}^{-2} \text{ s}^{-1}$	n.c.		n.c.			11.8		9.77		20.61
g CH <sub>4</sub> m <sup>-2</sup>	n.c.		n.c.			0.96		1.85		1.97
g CH <sub>4</sub> -C m <sup>-2</sup>	n.c.		n.c.			0.72		1.39		1.48
Global warming potential in g CO <sub>2</sub> -eq. m <sup>-2</sup>	n.c.		n.c.			<b>26.88</b>		<b>51.8</b>		<b>55.16</b>
% of the total budget	n.c.		n.c.			<b>1</b>		<b>2.3</b>		<b>1.9</b>
Average N <sub>2</sub> O flux $\text{nmol m}^{-2} \text{ s}^{-1}$	<i>0.84</i>		<i>0.25</i>			3.13	0.28	0.32		0.32
STDEV Average N <sub>2</sub> O flux $\text{nmol m}^{-2} \text{ s}^{-1}$	<i>0.84</i>		<i>0.2</i>			4.35	0.6	0.73		0.68
g N <sub>2</sub> O m <sup>-2</sup>	<i>1.17</i>		<i>0.34</i>			4.36	0.39	0.45		0.45
g N <sub>2</sub> O-N m <sup>-2</sup>	<i>0.74</i>		<i>0.22</i>			2.77	0.25	0.28		0.28
Global warming potential in g CO <sub>2</sub> -eq. m <sup>-2</sup>	<b>310.05</b>		<b>90.1</b>			<b>1155.4</b>	<b>103.35</b>	<b>119.25</b>		<b>119.25</b>
% of the total budget	<b>30.8</b>		<b>8.4</b>			<b>43.9</b>	<b>5.4</b>	<b>4.1</b>		<b>4.1</b>
Total GWP potential	<b>-385.18</b>		<b>-888.06</b>			<b>2629.44</b>	<b>-1892.65</b>	<b>-1876.75</b>		<b>-2577.25</b>

**Table 3:** Average GHG flux rates per season: winter (DJF), spring (MAM), summer (JJA) and fall (SON). Values are based on gap-filled data to avoid bias from missing nighttime data (predominantly relevant for CO<sub>2</sub>). Data are only presented when continuous measurements (eddy covariance data) were available. Sign convention: positive values denote export/release, negative

	CO <sub>2</sub> ( $\mu\text{mol m}^{-2} \text{s}^{-1}$ )				CH <sub>4</sub> ( $\text{nmol m}^{-2} \text{s}^{-1}$ )				N <sub>2</sub> O ( $\text{nmol m}^{-2} \text{s}^{-1}$ )			
	DJF	MAM	JAJ	SON	DJF	MAM	JAJ	SON	DJF	MAM	JAJ	SON
<b>2010</b>	0.56	-1.75	-0.79	0.01								
<b>SD</b>	5.39	12.07	11.34	9.31								
<b>2011</b>	0.48	-4.29	0.39	0.66								
<b>SD</b>	5.47	10.54	12.52	8.97								
<b>2012</b>	0.98	3.64	-0.33	-0.13	2.2	1.38	2.76	1.32	3.1	5.61	3.06	0.73
<b>SD</b>	5.69	9.1	13.65	8.03	14.91	11.85	10	9.94	4.77	5.52	3.19	0.92
<b>2013</b>	-0.2	-4.49	-1.3	0.13	2.18	5.3	3.79	3.4	0.12	0.19	0.73	0.26
<b>SD</b>	5.04	12.98	12.14	9.81	11.31	9.25	9.08	9.21	0.23	0.37	1.27	0.38
<b>2014</b>	-0.42	-5.07	-2.43	0.04	6.71	5.49	0.08	3.47	0.18	0.4	0.45	0.27
<b>SD</b>	6.56	12.93	12.98	9.45	22.93	31.37	8.5	10.21	0.27	0.78	0.87	0.63
<b>2010-2014</b>	0.28	-2.39	-0.89	0.14	3.69	4.06	2.21	2.73	1.14	2.07	1.42	0.42
<b>SD</b>	5.68	12.06	12.58	9.14	17.15	20.11	9.31	9.81	3.09	4.08	2.35	0.71



**Table 4:** Carbon and nitrogen gains/losses through fertilization, harvest and GHGs for the Chamau (CH-Cha) site in 2010- 2014. Values are given in kg ha<sup>-1</sup>. Gains are indicated with "-" and losses/exports are indicated with "+". While management information was available for both parcels (A and B), flux measurements are an integrate of both parcels. n.c. = not calculated

	2010		2011		2012		2013		2014		Total 2010 - 2014	
	Carbon	Nitrogen	Carbon	Nitrogen	Carbon	Nitrogen	Carbon	Nitrogen	Carbon	Nitrogen	Carbon	Nitrogen
<b>Fertilizer (kg ha<sup>-1</sup>) - Parcel A</b>	-1425.53	-253.09	-1222.06	-253.97	-2242.51	-271.12	-926.81	-213.19	-385.04	-122.08	-6201.95	-1113.45
<b>Fertilizer (kg ha<sup>-1</sup>) - Parcel B</b>	-1487.1	-194.3	-1509.9	-258.3	-2229	-293.2	-1001.1	-240	-996.8	-183.2	-7223.9	-1169
<b>Harvest (kg ha<sup>-1</sup>) - Parcel A</b>	3449.26	221.85	2570.3	165.32	1684.88	108.37	4393.9	282.61	3527.29	226.87	15625.63	1005.02
<b>Harvest (kg ha<sup>-1</sup>) - Parcel B</b>	2018.6	129.8	1952.2	125.6	1481.2	95.3	4174.8	268.5	6673.4	429.2	16300.2	1048.4
<b>Flux (CO<sub>2</sub>-C kg ha<sup>-1</sup>)</b>	-1896.6		-2667.7		3946.8		-5584.9		-7504.5		-13706.9	
<b>Flux (CH<sub>4</sub>-C kg ha<sup>-1</sup>)</b>	n.c.		n.c.		7.2		13.9		14.8		35.9	
<b>Flux (N<sub>2</sub>O-N kg ha<sup>-1</sup>)</b>		7.4		2.2		27.7		2.8		2.8		42.9
<b>Total - Parcel A</b>	<b>127.13</b>	<b>-23.84</b>	<b>-1319.46</b>	<b>-86.45</b>	<b>3396.37</b>	<b>-135.05</b>	<b>-2103.91</b>	<b>72.22</b>	<b>-4347.45</b>	<b>107.59</b>	<b>-4247.32</b>	<b>-65.53</b>
<b>Total - Parcel B</b>	<b>-1365.1</b>	<b>-57.1</b>	<b>-2225.4</b>	<b>-130.5</b>	<b>3206.2</b>	<b>-170.2</b>	<b>-2397.3</b>	<b>31.3</b>	<b>-1813.1</b>	<b>248.8</b>	<b>-4594.7</b>	<b>-77.7</b>

**Table 5:** Existing studies investigating the GHG exchange over pastures following ploughing. Results presented show the flux magnitude following ploughing and are rounded values of the individual presented in the papers. Values were converted to similar units (mg CO<sub>2</sub>-C m<sup>-2</sup> h<sup>-1</sup>, µg CH<sub>4</sub>-C m<sup>-2</sup> h<sup>-1</sup> and µg N<sub>2</sub>O-N m<sup>-2</sup> h<sup>-1</sup>). Based on Web of Knowledge search July 15th 2017 with the search terms "grassland", "pasture", "greenhouse gas", "ploughing" and/or "tillage". Only two studies representing conversion from pasture to cropland or other systems were included in this table.

Publication	Grassland type	Observation Period	Measurement technique	CO <sub>2</sub> -C	CH <sub>4</sub> -C	N <sub>2</sub> O-N	Supporting Information
Bertora et al. 2007	permanent pasture	62 days approx five years	Incubation study of soil cores	188 - 330 mg kg <sup>-1</sup> soil *	NA	50 - 1000 µg kg <sup>-1</sup> soil *	Simulated ploughing, varying moisture contents, earthworm fertilizer application between 36 - 133 kg N ha <sup>-1</sup> yr <sup>-1</sup> , conversion to cropland
Li et al. 2015	managed grassland	three years of cropland	static GHG chamber	> 600 mg m <sup>-2</sup> h <sup>-1</sup> &	NA	> 1000 µg m <sup>-2</sup> h <sup>-1</sup> &	15N gas flux method, restoration, two soil types, conversion to two soil types, N <sub>2</sub> O emissions and N leaching
Buchen et al. 2016	managed grassland	44 days	15N isotopic measurements	NA	NA	100 - 1000 µg m <sup>-2</sup> h <sup>-1</sup> ^	two soil types, N <sub>2</sub> O emissions and N leaching
Krol et al. 2016	permanent grassland	17 weeks	static GHG chambers on lysimeter	NA	NA	3000 µg m <sup>-2</sup> h <sup>-1</sup> %	two adjacent fields (tilled and untilled)
Cowan et al. 2016	permanent grassland	175 days	eddy covariance	NA	NA	500 - 700 µg m <sup>-2</sup> h <sup>-1</sup> \$	comparing ploughed and unploughed grassland
Drewer et al. 2016	permanent grassland poorly drained	three years	static GHG chambers/eddy covariance	250 - 2000 mg m <sup>-2</sup> h <sup>-1</sup> §	1000 - 8000 µg m <sup>-2</sup> h <sup>-1</sup> §	500 - 7000 µg m <sup>-2</sup> h <sup>-1</sup> §	grassland converted to fallow three treatments with different fertilizer levels, N <sub>2</sub> O and N <sub>2</sub> restoration occurring after two years
MacDonald et al. 2011	grassland		static GHG chambers	NA	NA	> 6000 µg m <sup>-2</sup> h <sup>-1</sup> !	grassland converted to fallow three treatments with different fertilizer levels, N <sub>2</sub> O and N <sub>2</sub> restoration occurring after two years
Estavillo et al. 2001	permanent pasture		incubation study of soil cores	NA	NA	1800 - 5000 µg m <sup>-2</sup> h <sup>-1</sup> §	grassland converted to fallow three treatments with different fertilizer levels, N <sub>2</sub> O and N <sub>2</sub> restoration occurring after two years
Merbold et al. 2014 and this study	permanent grassland	five years	static GHG chambers/eddy covariance	> 400 mg m <sup>-2</sup> h <sup>-1</sup> #	non-different from zero	> 2000 µg m <sup>-2</sup> h <sup>-1</sup> #	years

\* cumulative fluxes over 62 days, & conversion from grassland to cropland, ^ approximate value recalculated from figure in the paper, % approximate peak emission following restoration calculated from figure in the paper, § approximate value recalculated from figures presented in both paper, ! approximate value recalculated from figure in the paper, § approximate value presented in Figure 3 in the publication, # peak emissions

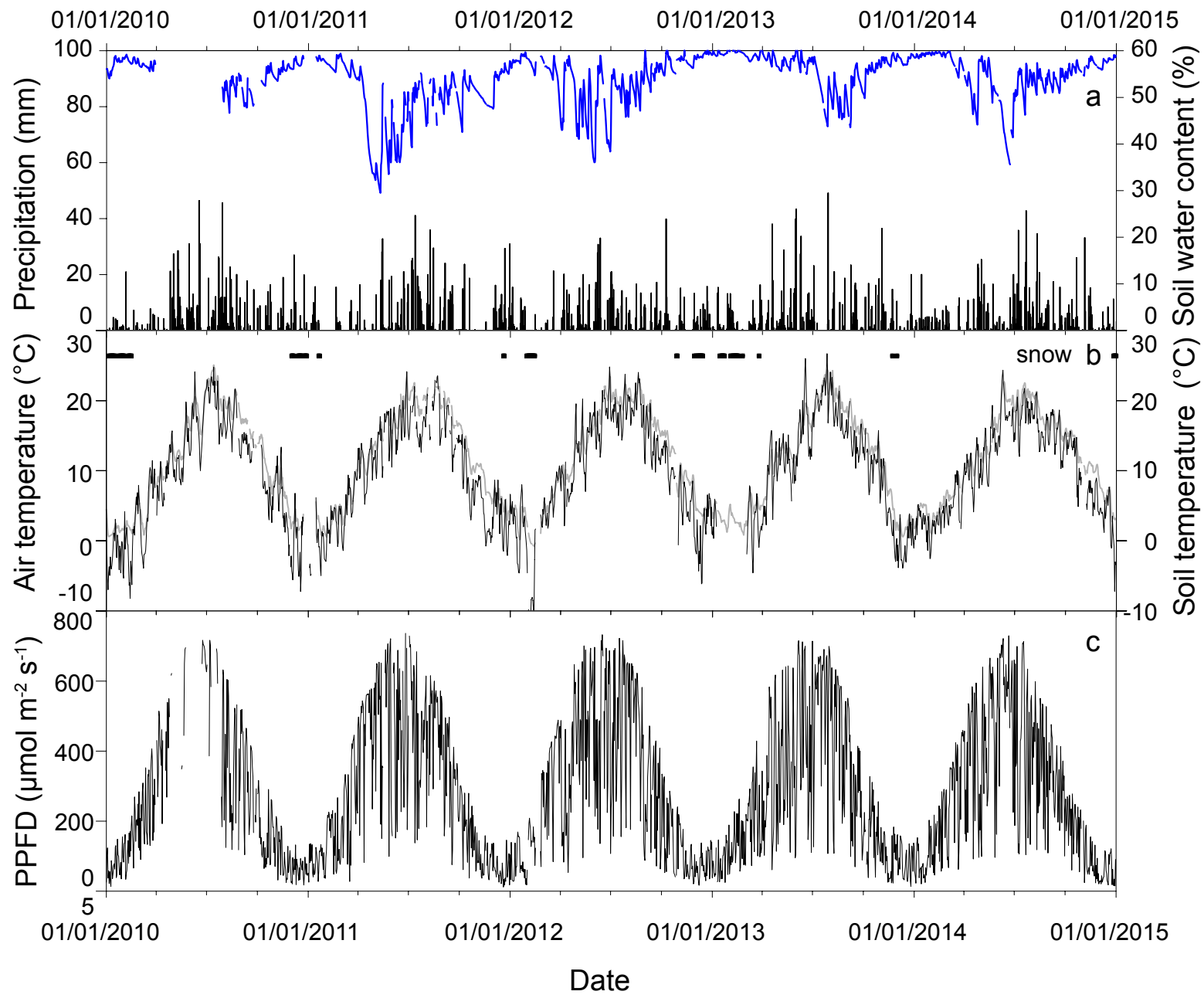


**Figure 1:** Weather conditions during the years 2010 – 2014. Weather data were measured with our meteorological sensors installed on site. (a) Daily sum of precipitation (mm) and soil water content (blue line, %) measured at 5 cm soil depth; (b) daily averaged air temperature (black line, °C), daily averaged soil temperature (grey line, °C), and days with snow cover (horizontal bars); (c) daily averaged photosynthetic photon flux density (PPFD,  $\mu\text{mol m}^{-2} \text{s}^{-1}$ ). Snow covered days were identified with albedo calculations. Days with albedo values  $> 0.45$  were identified as days with either snow or hoarfrost cover.

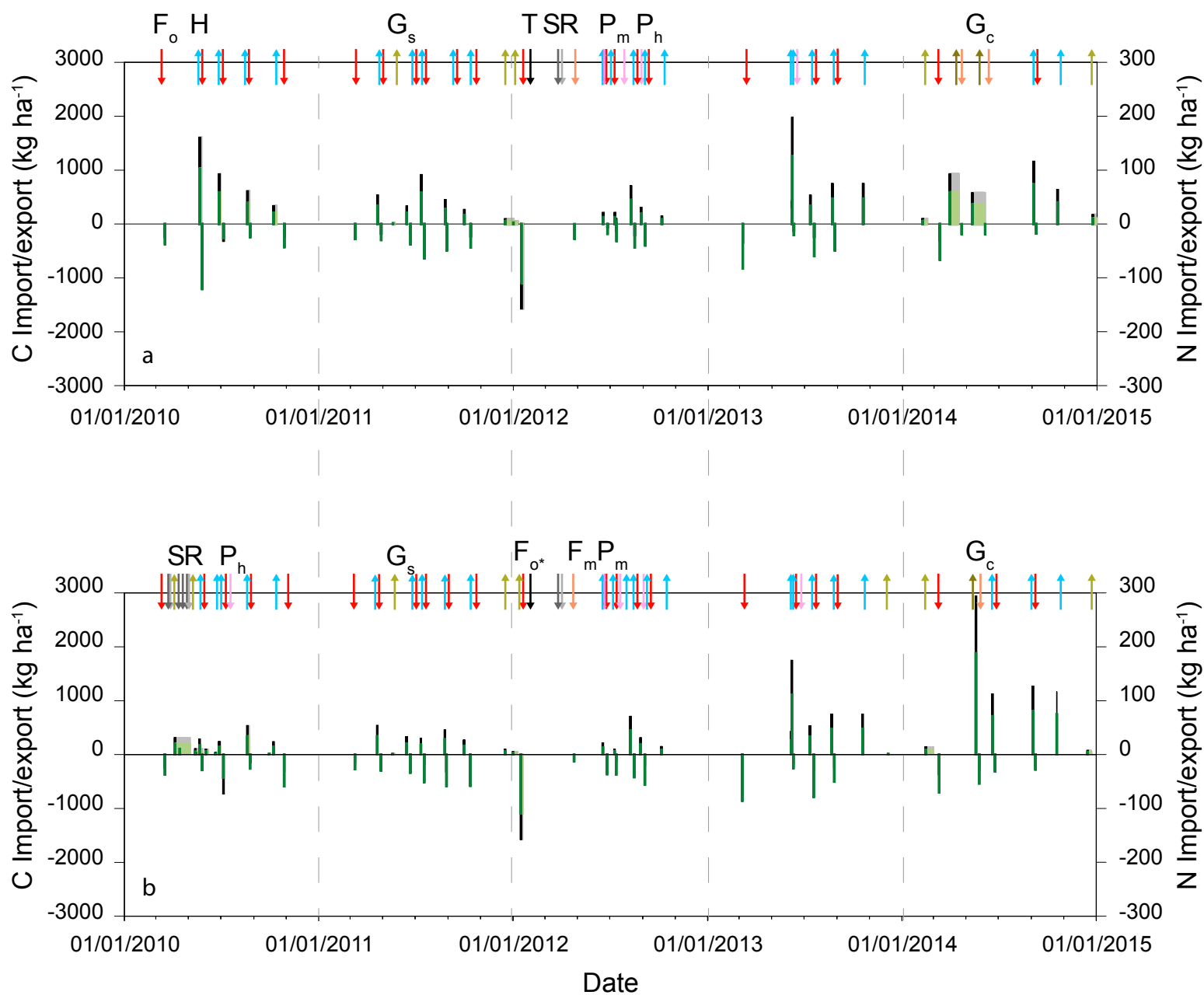


**Figure 2:** Management activities for both parcels (A and B in panels (a) and (b), respectively) on the CH-Cha site. Overall management varied particularly in 2010 between both parcels, whereas similar management took place between 2011 and 2014. Arrow direction indicates whether carbon (C in kg ha<sup>-1</sup>) and/or nitrogen (N in kg ha<sup>-1</sup>) were amended to, or exported from the site ("F<sub>o</sub>" and "F<sub>o\*</sub>"- organic fertilizers, slurry/mannure (red); "F<sub>m</sub>" - mineral fertilizer (light orange); "H" - harvest (light blue); "G<sub>s</sub>" and "G<sub>c</sub>" - grazing with sheep/cows (light/dark brown). Other coloured arrows visualize any other management activities such as pesticide application ("P<sub>h</sub>"- herbicide (light pink); "P<sub>m</sub>"- molluscicide (dark pink); "T"- tillage (black), "R"- rolling (light grey) and "S"- sowing (dark grey) which occurred predominantly in 2010 (parcel B) and 2012 (parcels A and B). Carbon imports and exports are indicated by black and grey bars. Thereby black indicated the start of the specific management activities and grey the duration (e.g. during grazing, "G<sub>s</sub>"). Green colors indicate nitrogen amendments or losses, with dark green visualizing the start of the activity and light green colors indicating the duration. Sign convention: positive values denote export/release, negative values import/uptake.

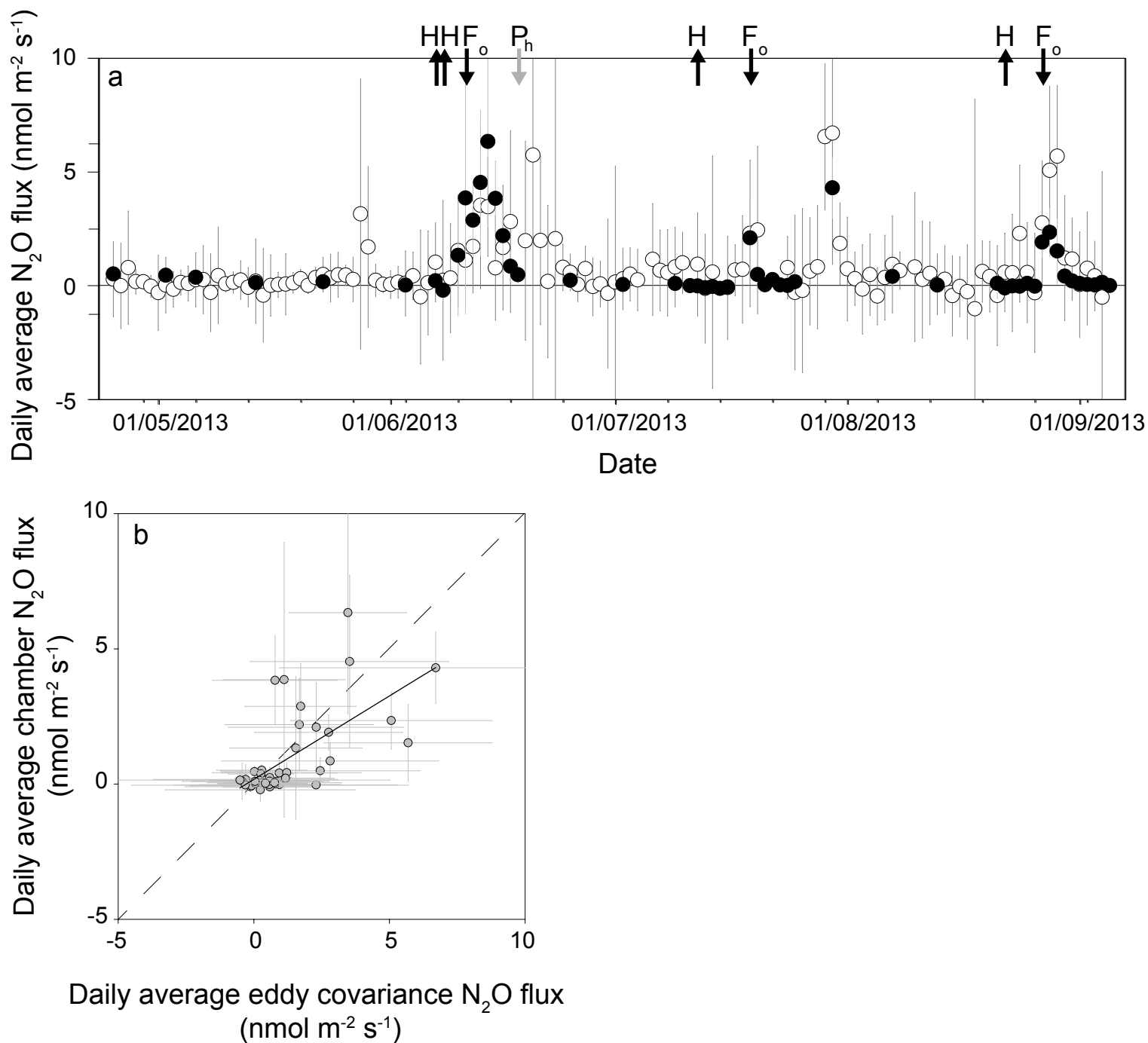


**Figure 3:** (a) Temporal dynamics of daily average  $N_2O$  fluxes measured with the eddy covariance (white circles) and manual greenhouse gas chambers (black circles) in 2013. Black arrows indicate management events, grey lines indicate standard deviation ("H"= harvest, "F<sub>o</sub>"= organic fertilizer application (slurry), "P<sub>h</sub>"= pesticide (herbicide) application); (b) 1:1 comparison between chamber based and eddy covariance based  $N_2O$  fluxes in 2013. The dashed line represents the 1:1 line. (Regression:  $y = 0.61x + 0.17$ ,  $r^2 = 0.4$ ). Sign convention: positive values denote export/release, negative values import/uptake.

